

TNO report
FEL-98-A077

Geographical information extraction with remote sensing Part I of III - Main report

TNO Physics and Electronics
Laboratory

Oude Waalsdorperweg 63
PO Box 96864
2509 JG The Hague
The Netherlands

Phone +31 70 374 00 00
Fax +31 70 328 09 61



All information which is classified according to Dutch regulations shall be treated by the recipient in the same way as classified information of corresponding value in his own country. No part of this information will be disclosed to any third party.

The classification designation Ongerubriceerd is equivalent to Unclassified, Stg. Confidentieel is equivalent to Confidential and Stg. Geheim is equivalent to Secret.

All rights reserved. No part of this report may be reproduced in any form by print, photoprint, microfilm or any other means without the previous written permission from TNO.

In case this report was drafted on instructions from the Ministry of Defence the rights and obligations of the principal and TNO are subject to the standard conditions for research and development instructions, established by the Ministry of Defence and TNO, if these conditions are declared applicable, or the relevant agreement concluded between the contracting parties.

© 1998 TNO

DTIC QUALITY INSPECTED 1

The TNO Physics and Electronics Laboratory is part of TNO Defence Research which further consists of:

TNO Prins Maurits Laboratory
TNO Human Factors Research Institute

Date
August 1998

Author(s)
Dr A.C. van den Broek
M. van Persie
H.H.S. Noorbergen
Dr G.J. Rijckenberg

Sponsor HWO-CO/HWO-KL
Project officer J. Rogge
Affiliation KMA

Classification
Classified by J. Rogge
Classification date 18 August 1998

Title Ongerubriceerd
Managementuittreksel Ongerubriceerd
Abstract Ongerubriceerd
Report text Ongerubriceerd

Copy no 12
No of copies 54
No of pages 94 (excl RDP & distribution list)
No of appendices -

DISTRIBUTION STATEMENT A
Approved for public release;
Distribution Unlimited

19990126 149



AQF99-04-0710
Netherlands Organization for
Applied Scientific Research (TNO)

REPRODUCTION QUALITY NOTICE

This document is the best quality available. The copy furnished to DTIC contained pages that may have the following quality problems:

- **Pages smaller or larger than normal.**
- **Pages with background color or light colored printing.**
- **Pages with small type or poor printing; and or**
- **Pages with continuous tone material or color photographs.**

Due to various output media available these conditions may or may not cause poor legibility in the microfiche or hardcopy output you receive.



If this block is checked, the copy furnished to DTIC contained pages with color printing, that when reproduced in Black and White, may change detail of the original copy.

Managementuittreksel

Titel : Geographical information extraction with remote sensing
Part I of III - Main report
Auteur(s) : Dr. A.C. van den Broek, Ir. M. van Persie,
Ing. H.H.S. Noorbergen, Dr. G.J. Rijkenberg
Datum : augustus 1998
Opdrachtnr. : A95KL756
IWP-nr. : -
Rapportnr. : FEL-98-A077

Achtergrond

Door de veranderende omstandigheden na het einde van de koude oorlog zijn de taken van de Nederlandse Krijgsmacht ingrijpend gewijzigd. Tegenwoordig overweegt de Krijgsmacht deelname aan en is de Krijgsmacht ook daadwerkelijk betrokken bij operaties buiten het eigenlijke NAVO gebied. Voor het NAVO gebied zelf is voldoende geografische informatie voorhanden, die bij NAVO acties door de verschillende NAVO partners onderling aan elkaar wordt doorgespeeld. Voor vele andere gebieden op de wereld is geografische informatie vaak schaars en/of verouderd. Voor niet NAVO acties zoals operaties in VN kader is elk land verantwoordelijk voor de eigen informatie voorziening. In dit kader is een onafhankelijke en toegankelijke bron voor geografische informatie een noodzaak. Remote sensing informatie van satellieten, maar ook van vliegtuigen en UAV's kan zo'n bron voor geografische informatie zijn.

Doelstelling

Doel van deze studie is het evalueren van de mogelijkheden die remote sensing data bieden om geografische informatie te verkrijgen. De verkregen geografische informatie kan gebruikt worden om een onbekend gebied in kaart te brengen dan wel oudere kaarten van een update te voorzien. Om bovengenoemd doel te verwezenlijken is remote sensing data verzameld van sensoren uit verschillende golflengte gebieden (optisch, thermisch infrarood en microgolf) gedragen door verschillende platformen (vliegtuigen en satellieten) waarop deze sensoren zich bevinden. De remote sensing data hebben betrekking op twee testgebieden, die beide een verscheidenheid aan geografische kenmerken laten zien.

Omschrijving van de werkzaamheden

Een van de testgebieden, genaamd het "Heerde testgebied" naar topografische kaart 27, is gelegen in Nederland en is nagenoeg vlak. Er is een digitale geografische database (TERAS: TERrein Analyse Systeem) beschikbaar, zodat een gedetailleerde vergelijking tussen de remote sensing data en de bestaande geografische informatie uit de database mogelijk is. Voor dit testgebied is een volledige collectie van remote sensing beelden aanwezig, die bestaat uit beelden afkomstig van de satellieten TM, SPOT, KVR, ERS en JERS en van de vliegtuigsensoren CAESAR, PHARS/PHARUS en TIR.

Gebruik makend van een lijst in DIGEST (Digital Geographical Information Exchange Standard) formaat met geografische voor militairen interessante kenmerken, is uit de beelden geografische informatie ge-extraheerd. De kenmerken hebben betrekking op de klassen cultuur (bebouwing, wegen, bruggen e.d.), hydrografie (waterlopen, duikers, meren e.d) en vegetatie/landvormen (landbouwwelden, bossen e.d.). Om de ge-extraheerde informatie te evalueren voor het doel van cartografie hebben we deze vergeleken met de TERAS database voor het Heerde gebied. De TERAS database bevat data in GIS (vector) formaat die vergelijkbaar is met een topografische kaart met schaal 1:50.000.

Het tweede testgebied is gelegen in Duitsland nabij Freiburg en omvat zowel de Rijn Vallei als het Zwarte Woud dat middelgebergte tot 1500 m bevat. Voor dit testgebied is gebruik gemaakt van satelliet data afkomstig van TM, SPOT, ERS, JERS en KVR. Tevens is er een digitaal hoogte model (DTED) beschikbaar. Dit testgebied is vooral gebruikt om de invloed van het reliëf op de remote sensing beelden te bestuderen. Tevens is bestudeerd hoe een digitaal hoogte-model uit de beelden kan worden gegenereerd.

Resultaten en conclusies

Het is moeilijk om algemene conclusies te trekken voor alle beschouwde kenmerken omdat de karakteristieken van elk kenmerk nogal verschillend zijn. Elk kenmerk moet daarom meestal op zichzelf staand worden beoordeeld. Door de kenmerken groepsgewijs te beschouwen kunnen wel enige algemene conclusies getrokken worden, omdat de meeste cultuur kenmerken punten in het beeld zijn en vele vegetatie/landvorm kenmerken uit polygonen bestaan.

In het algemeen kan men zeggen dat de meeste kenmerken uit de DIGIST lijst zowel gedetecteerd als herkend kunnen worden als de resolutie en golflengte geschikt gekozen zijn. Zo kunnen "man-made" kenmerken als gebouwen of wegen gedetecteerd en vaak ook herkend worden met een resolutie in de orde van 5 meter of kleiner. Met resoluties in de orde van 1 meter of kleiner kunnen de meeste kenmerken herkend worden. Voor in oppervlakte uitgebreide kenmerken (polygonen), zoals landbouwgrond of bos is spectrale/polarimetrische informatie belangrijker dan resolutie.

Sommige kenmerken zoals uiterwaarden en grondwater zijn moeilijk om met remote sensing sensoren direct waar te nemen. Toch kan informatie omtrent deze kenmerken verkregen worden door andere kenmerken waar te nemen die met de eerste in verband staan. We noemen dit hier "context" informatie, bijvoorbeeld de aanwezigheid van groene vegetatie duidt op de aanwezigheid van grondwater.

We geven hier onze bevindingen voor sensoren in het optisch, thermisch infrarood en microgolf gebied afzonderlijk:

Optische sensoren maken gebruik van daglicht en zijn afhankelijk van het weer. Optische sensoren kunnen hoge resolutie (< 1 meter) beelden af leveren, zodat kenmerken in het algemeen gemakkelijk herkend kunnen worden. Radiometrische resolutie (het aantal grijs tinten) en spectrale informatie zijn echter mede bepalend voor het resultaat. Dit laatste is vooral het geval om bijvoorbeeld gebouwen en

wegen te kunnen onderscheiden van het omliggende gebied. Nabij-infrarood informatie is vooral belangrijk om typen vegetatie te kunnen onderscheiden. *Thermisch infrarood (TIR) sensoren* zijn bijzonder geschikt om 'man-made' kenmerken te detecteren en te herkennen als de weersomstandigheden goed zijn. In het algemeen is dit helder en zonnig weer. De weersomstandigheden zijn echter cruciaal voor het resultaat. Gedurende een bewolkte, mistige of regenachtige dag kan het contrast volkomen verdwijnen, zodat de kenmerken nauwelijks meer zichtbaar zijn. Voor het onderscheiden van verschillende soorten vegetatie zijn TIR sensoren minder geschikt.

Het grote voordeel van *microgolf sensoren* is dat zij onafhankelijk van de weersomstandigheden en op elk tijdstip van dag en nacht kunnen worden ingezet, omdat zij zelf straling uitzenden. Microgolf sensoren zijn geschikt voor detectie van vooral man-made kenmerken omdat hierbij vaak een helder punt in het beeld te zien is vanwege zogenaamde speculaire (spiegelende) reflecties. Een voorbeeld zijn hoogspanningsmasten die in ERS beelden te zien zijn, terwijl de resolutie, zelfs te laag zou zijn in het optische geval.

Kenmerken herkennen is echter moeilijker in microgolf beelden, zelfs als de resolutie hoog genoeg is. De omtrek van objecten die in optische en TIR beelden te zien is ontbreekt meestal in microgolf beelden door toedoen van speckle (ruis) en speculaire reflecties, hetgeen de herkenning bemoeilijkt.

De lage resolutie van de hedendaagse microgolf satellieten zoals de ERS is duidelijk een nadeel om ze te gebruiken voor militaire cartografie.

Een belangrijk begrip in verband met detectie en herkenning is zogenaamde context informatie. De context kan namelijk informatie verschaffen omtrent een kenmerk zonder dat het direct gezien wordt. Vaak worden kenmerken waargenomen als een punt of een paar punten in het beeld zodat directe herkenning niet mogelijk is. Soms echter is er onafhankelijke "achtergrond" informatie beschikbaar voor de interpretator, zodat deze het kenmerk toch kan herkennen. Deze "context" of "achtergrond" informatie speelt altijd een belangrijke rol bij het interpreteren van remote sensing beelden. Het is op die manier mogelijk veel meer informatie uit de beelden te halen dan men zou verwachten.

We concluderen dat zowel in optische als microgolf gebied het reliëf de beelden zowel geometrisch als radiometrisch verstoort. Alleen wanneer verticaal gekeken wordt is er bij optische beelden geen verstoring. Voor microgolf beelden geldt dit niet omdat altijd zijwaarts gekeken moet worden om een beeld op te nemen. De verstoringen kunnen echter gebruikt worden in zogenaamde stereo paren om hoogte informatie te extraheren. Op deze manier kan in principe een digitaal hoogte model gecreëerd worden. Met behulp van satelliet SPOT stereo data was het mogelijk een hoogte nauwkeurigheid van 10 meter te verkrijgen.

Met microgolf sensoren is het ook mogelijk om een dergelijke hoogte nauwkeurigheid te halen wanneer twee opnamen tegelijkertijd gemaakt worden vanuit een enigszins andere positie. Een dergelijk instrument is momenteel nog niet beschikbaar in de ruimte maar met vliegtuigen zijn al goede resultaten behaald.

Contents

1.	Introduction.....	7
2.	The remote sensing data-set.....	9
2.1	Heerde test site	9
2.2	Description of the Heerde data.....	10
2.3	Freiburg test site	32
2.4	Description of the Freiburg data.....	32
3.	The ground database (TERAS).....	51
4.	Comparison of the ground database with the remote sensing data-set	57
4.1	Introduction	57
4.2	The remote sensing data used.....	57
4.3	Method of comparison.....	57
4.4	Results of the comparison	58
4.5	Other comparisons with remote sensing data.....	61
4.6	Estimation of the resolution required for obtaining geographical information.....	62
5.	Relief.....	67
5.1	Influence of relief on remote sensing images.....	67
5.2	DEM generation from remote sensing images	76
6.	Conclusions.....	87
6.1	General	87
6.2	Comparison between the sensors	87
6.3	Context	88
6.4	Relief	88
7.	References.....	91
8.	Signature	93

1. Introduction

Background

Due to the changing international situation after 1989 the tasks of the Royal Netherlands Army (RNLA) have changed considerably. Nowadays the RNLA considers and carries out operations outside the actual NATO area contrasting the situation during the Cold War. For NATO areas geographical information is sufficiently available and this information is shared in case of allied operations. For many other parts of the world geographical information is often sparse, and for non-NATO operations like UN operations each country is responsible for its own intelligence. In this context an independent and accessible source of geographical information is a necessity. Remote sensing data from satellites, but also from aeroplanes or UAV's offer such a source for geographical information.

Goal

The goal of this study is to evaluate the potential of remote sensing for geographical information extraction. The extracted information can then be used to update outdated maps or to obtain basic information about an unknown site.

Scope

In this study we have collected remote sensing data from sensors in different wavelength regions (optical, thermal infrared and microwave) and from different platforms (spaceborne as well as airborne).

This has been done for two test sites showing a variety of geographical features. One test site, located in the Netherlands, shows no significant relief. For this test site a digital geographical database is available, so that a detailed comparison between the remote sensing data and the geographical database is possible. A second test site, located in Germany, shows relief up to 1500 meter and is used to study the influence of relief on remote sensing images and the generation of a digital elevation model (DEM) from these images.

Organisation of the report

The report consists of four parts.

1. Main report In the main report we describe the adopted method and summarise the data. We furthermore present the results of the comparison

between the extracted geographical data from the sensors and the ground data. We also discuss the reliability of the extracted information. Finally we summarise our conclusions.

2. Technical Supplement In the Technical Supplement we give detailed information about sensors and image data. We discuss extraction and visualisation techniques.
3. Appendix We give here lists of geographical features and attributes used in this study. We furthermore summarise and explain keywords and technical expressions used in the study.
4. Image catalogue In the image catalogue we show images from the different sensors for every geographical feature studied.

2. The remote sensing data-set

For this study we have used remote sensing data from three wavelength domains (optical/near infrared, thermal infrared and microwave) and for two test sites. One test site is located in the Netherlands and is called the Heerde test site after the topographical map 27. For this test site a complete collection of remote sensing images consisting of TM, SPOT, KVR, ERS, JERS, CAESAR, PHARS and TIR data is available. The second test site is located in Germany near Freiburg and contains moderate relief. For this site, the Freiburg test site, TM, SPOT, ERS, JERS and KVR data, including a DEM are available.

In the next sections we give a detailed description of the sites and the remote sensing data which are available.

2.1 Heerde test site

The actual test site is oriented is exactly east-west, located on TDN topographical map 27, and comprises an area of 10 by 20 km between the river IJssel and the Holterberg to the North of the city Deventer. The location is given by RD co-ordinates (x, y) 200000, 477500 m (South West corner) and (x, y) 220000, 487500 m (North East corner). The test site is called the "Heerde" test area after the name for TDN topographical map 27, although the village "Heerde" is not located in the actual test site.

Low resolution satellite remote sensing data is available for the entire map 27 East and West (RD 180000,475000 (South West), RD 220000,500000 (North-East)), while high resolution airborne data are only available for the actual test site.

The test site includes the IJssel and its inundation (uiterwaarden) and shows landscapes like build-up areas, roads, forest, agricultural areas etc. The terrain is flat up to a few meters. For this area a complete set of images with resolutions ranging from 2 meters to 30 meters are available enabling a detailed comparison between the ground data and the extracted geographical information. Details of the data are given in Table 1.

Table 1: Sensor and image data properties for Heerde area.

<i>sensor</i>	<i>platform</i>	<i>resolution (m)</i>	<i>type</i>	<i>date (d-m-y)</i>	<i>time</i>
TM	spaceborne	30	optical/nir-multispectral	10-18-1993	11:10 (solar)
SPOT XS	spaceborne	20	optical- multispectral	10-06-1992	-
SPOT PAN	spaceborne	10	optical- panchromatic	13-10-1992	-
KVR1000	spaceborne	2	optical- photographic	19-05-1992	-
ERS-1	spaceborne	25 (3 looks)	microwave- C-band/VV/23°	06-08-1992 02-07-1992 23-06-1992	-
JERS-1	spaceborne	25 (3 looks)	microwave- L-band/HH/35°	20-09-1993	-
CAESAR	airborne	3	optical- multispectral	22-09-1994	13:44 (GMT) 14:01 (GMT) 14:18 (GMT) 14:45 (GMT) 15:01 (GMT)
PHARS	airborne	6 (8 looks)	microwave -C-band/VV/45-65°	27-09-1994	-
PHARUS	airborne	3 (5 looks)	microwave -C-band/Pol./50-70°	02-06-1997	-
TIR-camera	airborne	5	thermal infrared scanner	23-09-1994/ 14-10-1994	-

All data were co-registered to the topographical maps 27 East and 27 West, with ground control points and using a stereographical projection and a Bessel ellipsoid as is usual for the Netherlands. The central point of the projection is located in the city of Amersfoort (RD co-ordinates (x, y) 155000, 463000 or 52.2° lat., 5.5° long.). The accuracy of the registration is determined by the geometrical accuracy of the data and how accurately the ground control points can be determined with respect to the topographical map. This depends on the scale of the maps and on the resolution of the data. For the airborne data we used maps with a scale of 1:10,000, so that the data could be registered with an accuracy close to the dimension of the resolution cell. (i.e. 3 to 5 m). The satellite data could also be registered with accuracies within the dimensions of the resolution cell (i.e. 10 -30 m) using maps of 1:50,000. An exception are the KVR data which are registered with an accuracy of 10 m, while the resolution is 2 m. This is due to the lower geometrical accuracy of the KVR data.

2.2 Description of the Heerde data

For the low resolution spaceborne systems (TM, ERS and JERS) we show images of the whole area covering map 27 (East and West). For SPOT-PAN, CAESAR, PHARS we show images for the actual test area. For orientation and comparison we also show topographical maps (scale 1:50,000) of 27EW (Fig. 1) and the actual test area (Fig. 5). A detailed inspection of TIR, PHARS, CAESAR and KVR data is possible in Figs. 9 and 10, where we have printed an area of 2 by 3 km near the village of Olst (RD 203000, 482700 (South West), RD 206000, 484700 (North East)). In the following we give a concise description of the images collected by the sensors.



Figure 1: Topographical map 1:50,000 'Heerde'. Map no. 27W and 27E. The top is North as usual and the dimensions are 50 by 25 km. Actual scale on paper is 1:200,000.

TM

We show in Fig. 2 band 4, 5 and 3 in the red, green and blue channel respectively. This means that the red and green channel represent 2 near-infrared bands (1.6 and 0.8 micron). The blue channel represent the red band (0.6 micron) . Because vegetation reflects radiation very well at 0.8 micron compared to the other bands it colours green in the images. This is different for forest (dark green) and for grass (light green). For bare soil, and other materials like stone and brick, the reflection is relatively small at 0.8 micron, so that non-vegetated fields in the Flevoland polder, cities, roads etc. are coloured purple. Areas with sand (Veluwe) show some more reflection at 1.6 micron and are coloured reddish while water reflects better at 0.6 micron and shows a dark blue colour.

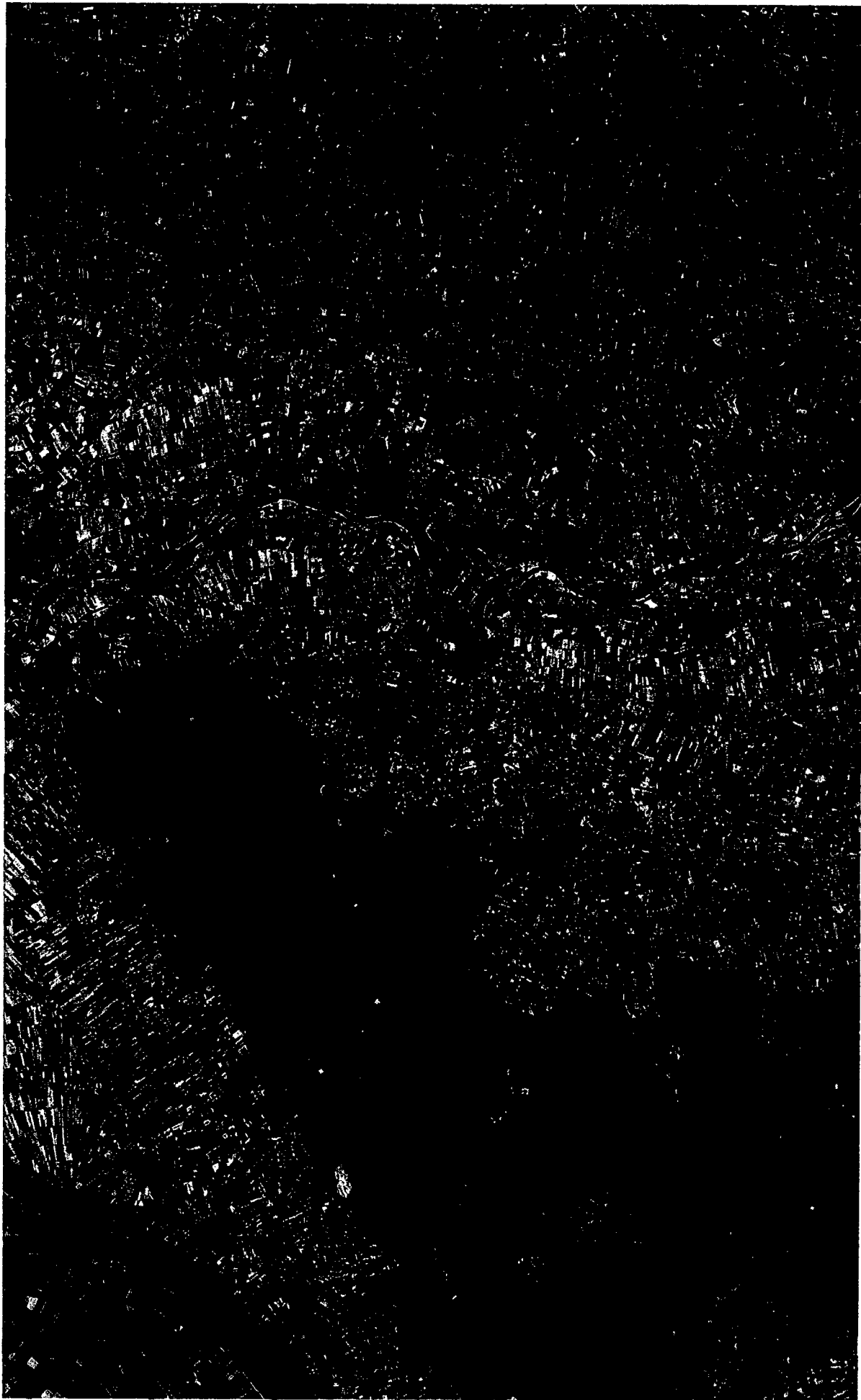


Figure 2: TM image of map 27W and 27E. Band 5 (1.6μ), 4 (0.8μ) and 3 (0.65μ) are shown in the red, green and blue channel respectively. Resolution is 30 m.

ERS

In this image (Fig. 3) forest shows up bright compared to bare soil and grass, since forested areas give more backscatter. High returns, due to double bounce reflections, are seen in cities, especially where big buildings like flats and industrial buildings are present. Water is also relatively bright since small waves generated by wind give considerable backscatter. The recognition of the river IJssel is therefore less easy. The bigger roads show up as black lines. Note that sometimes high tension lines show up which are indicated by a series of points in a row representing the high tension pylons and the wires.

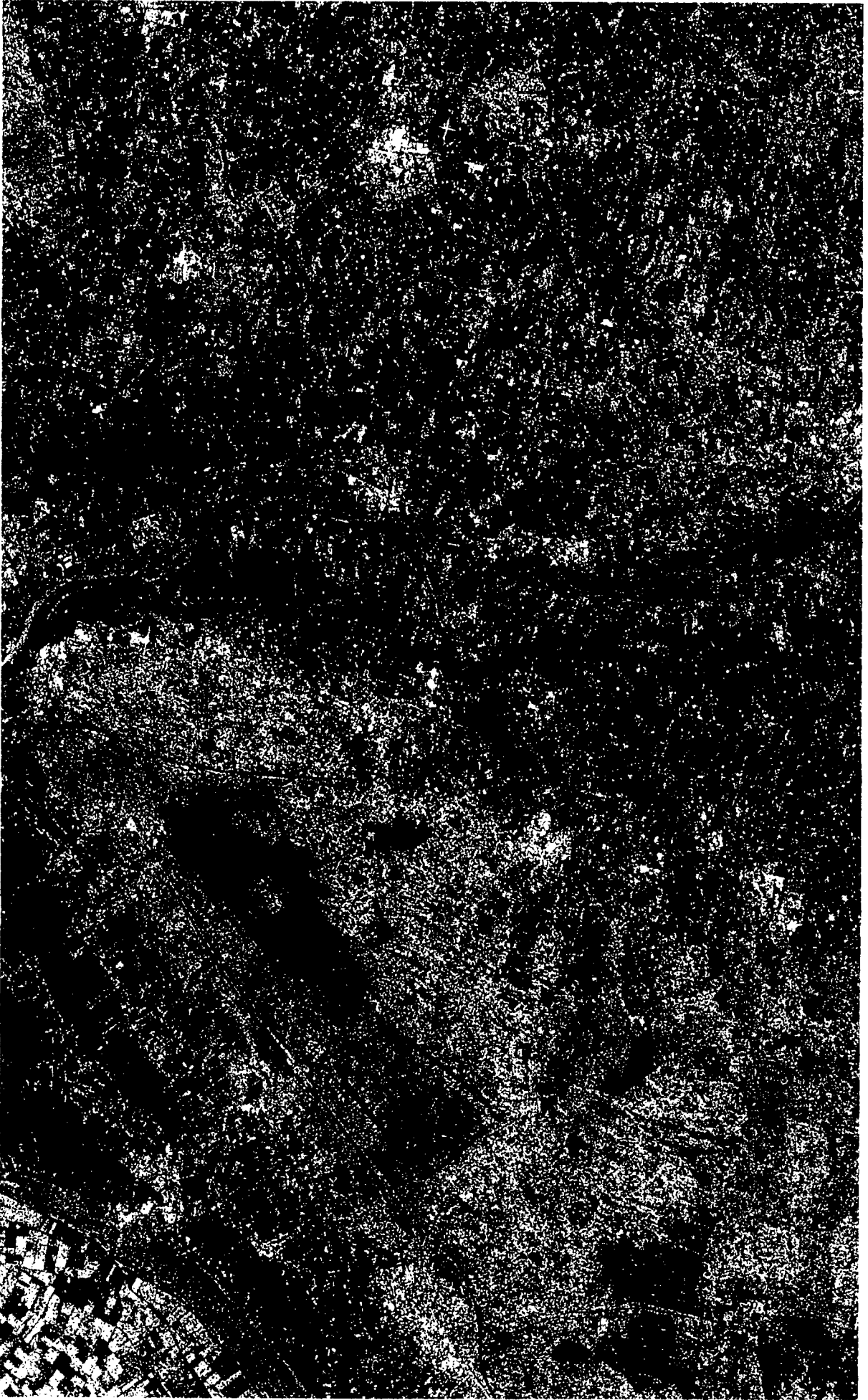


Figure 3: ERS image of map 27W and 27E. Resolution is 25 m, 3 looks. Wavelength is 5.3 cm (C-band), VV polarised, incidence angle is 23 degrees.

JERS

A JERS image is shown in Fig. 4. Compared to the ERS image the forested areas are even brighter while bare soil, grass and water are relatively dark. This is due to the longer wavelength (30 cm instead of 5.3 cm for ERS) and the larger incidence angle (40 degrees instead of 23 degrees for ERS), so that for fields and water the backscatter is decreased. This is not true for forested areas where a lot of scattering occurs. Double bounce reflections from big buildings indicate their presence similarly to the ERS. To the west of the river IJssel, which is now clearly visible as a winding line, high tension lines are clearly visible.

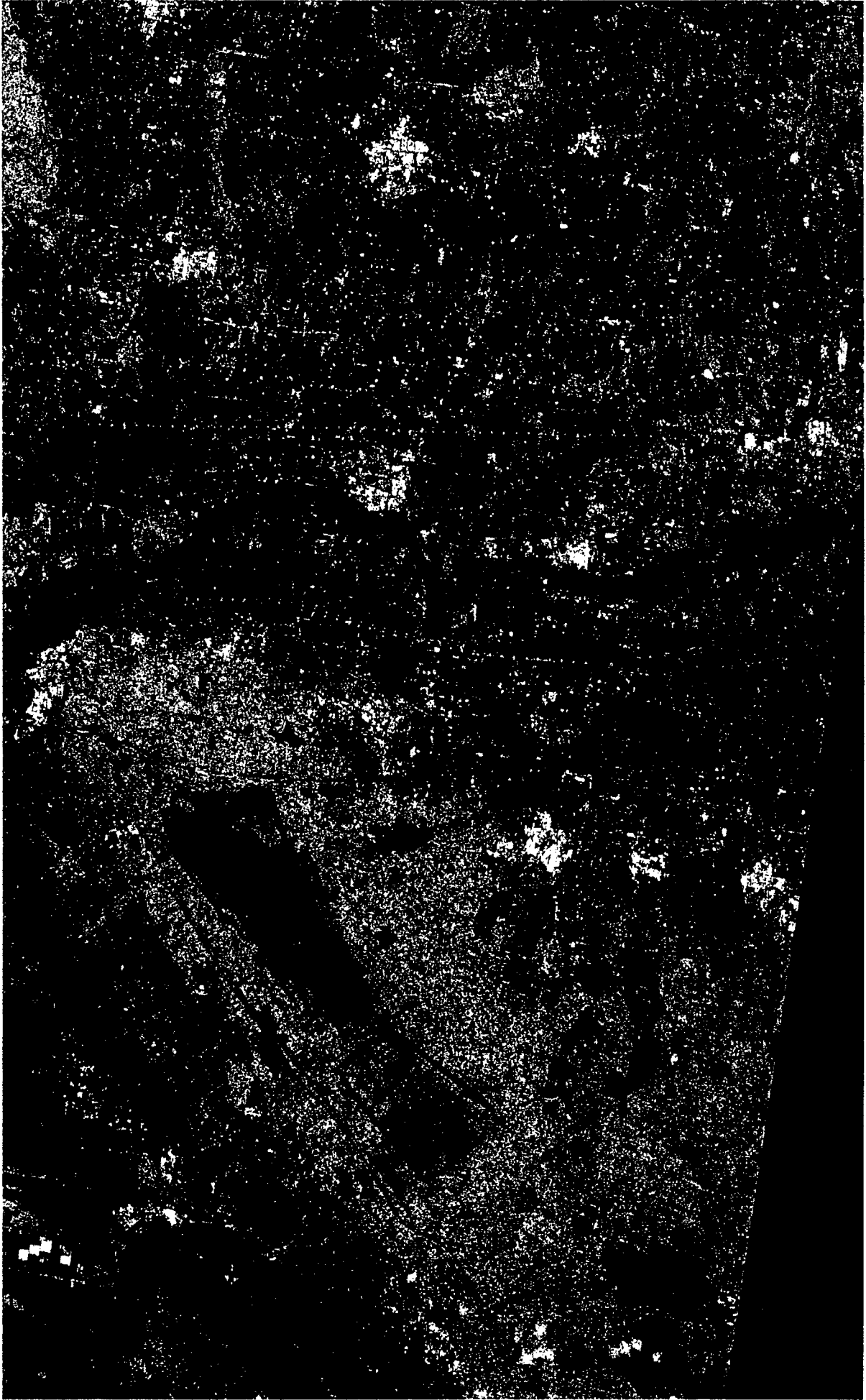


Figure 4: JERS image of map 27W and 27E. The SE corner was not available. Resolution is 25 m, 3 looks. Wavelength is 25 cm (L-band), HH polarised, incidence angle is 40 degrees.

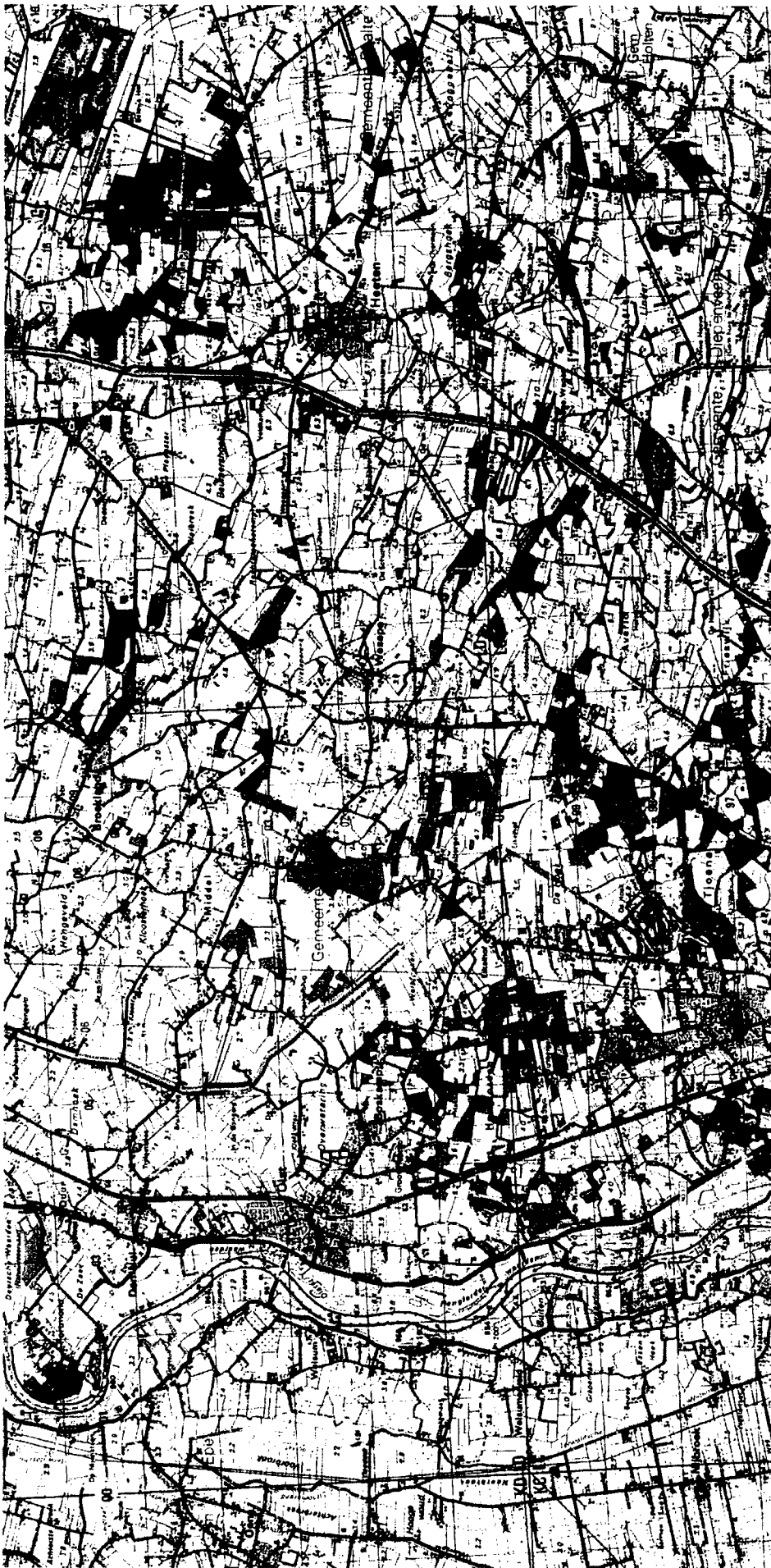


Figure 5: Topographical map 1:50,000 of the actual test area of 20 by 10 km. The area is aligned exactly West-East so that North is to the top. Actual scale on paper is 1:80,000.

SPOT-PAN

A SPOT-Pan image for the actual test area (Fig. 5) is shown in Fig. 6. During the recording of this black and white PAN image an optical window of 0.5 to 0.75 micron has been used. Most radiation is absorbed by the vegetation which therefore appears black. Bare soil, roads and houses reflect optical radiation much better so that they appear bright in the image. Low vegetated land like grass and water appears greyish.

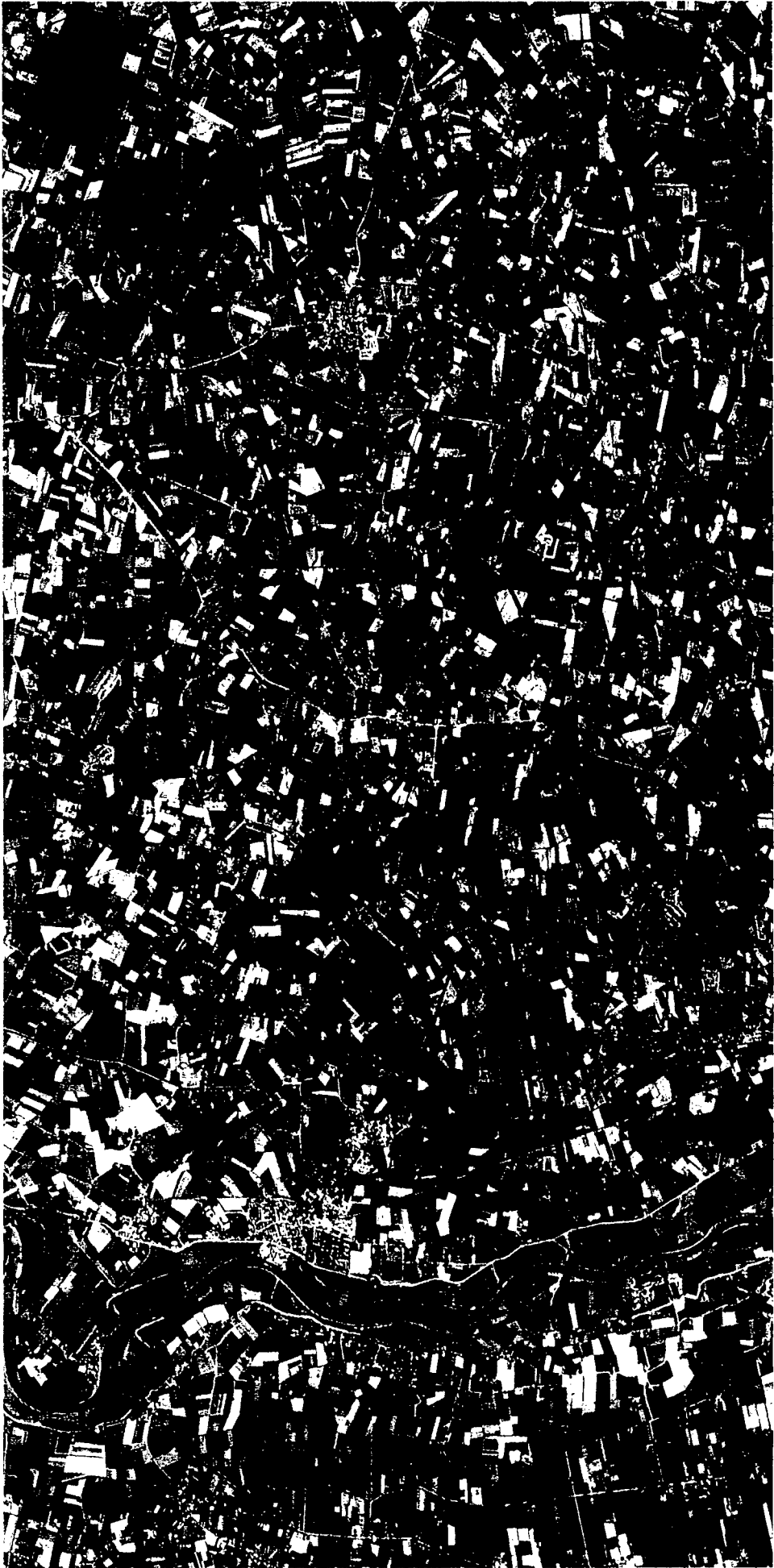


Figure 6: SPOT-PAN image of the test area. Optical imaging ($0.5\text{--}0.75\text{ }\mu$), resolution is 10 m.

CAESAR

In this image (Fig. 7) the three bands (near-infrared, red and green) are shown in the red, green and blue channel. Bare soil, roads and houses, which appear bright in the PAN image are now blue-green. Note that a direct comparison with the PAN image is not possible since the images are recorded in different years. The reflection of vegetation in the near-infrared band is quite strong so that vegetation appears reddish, contrary to the bare soil and the roads. Since different kinds of vegetation reflect the near-infrared radiation differently, they colour differently so that they can be discriminated. Forest is dark red. Grass is light red, while maize (full grown) is light brown. This image is a mosaic of 5 strips which still can be recognised. Furthermore some clouds and their shadows are visible.



Figure 7: CAESAR image of the test area. Band 1 (0.88 μ), 4 (0.67 μ) and 1 (0.55 μ) are shown in the red, green and blue channel. Resolution is 3 meter.

PHARS

A PHARS image is shown in Fig. 8a. Like in the case of ERS, which uses the same wavelength, trees and forest appear bright. Because of the higher resolution layover and shadow due to forest edges and rows of trees become visible, which facilitates their recognition. Also maize fields are relatively bright, while the grassland is relatively dark. Farms and the larger houses appear as clear point targets in the image. Large roads, channels and the IJssel appear as dark lines. Note that the railroad appears as a bright line due to reflection from the high tension pylons belonging to the railroad.



Figure 8a: PHARS image of the test area. Resolution is 6 meter, 7 looks. Wavelength is 5.3 cm, VV polarised. Incidence angle varies from 45 (North and South edge) to 65 degrees (middle). A strip in the NE corner was not available.

PHARUS

A PHARUS image is shown in Fig. 8b. This polarimetric image shows the HH, HV and VV polarisation in the red, green and blue colour channels, so that different types of land use give rise to different colours. In this colour representation bare soil fields are purple, grass fields green. Forest shows a bright greenish colour while urban areas show a reddish colour due to double bounce scattering (see section S1.3 of the Technical Supplement). Other colours like brown and bluish are usually related to other types of vegetation than the above mentioned types, like crops.



Figure 8b: PHARUS image of part of the test area. Resolution is about 4 meter, 5 looks. Wavelength is 5.3 cm. Polarimetric image showing the HH, HV and VV polarisation in the red, green and blue channels, respectively. Incidence angle varies from 45 (North edge) to 65 degrees (South edge).

KVR

The KVR image (Fig. 9) is comparable to the SPOT image, except that the resolution is much better so that more details can be seen. Since the KVR is not a digital instrument (it uses photographic film) the images show less grey levels than in the case of SPOT-PAN, reducing the radiometric resolution. Since most types of vegetation appear black discrimination especially between different types of fields is difficult despite the high geometric resolution of 2 meter.

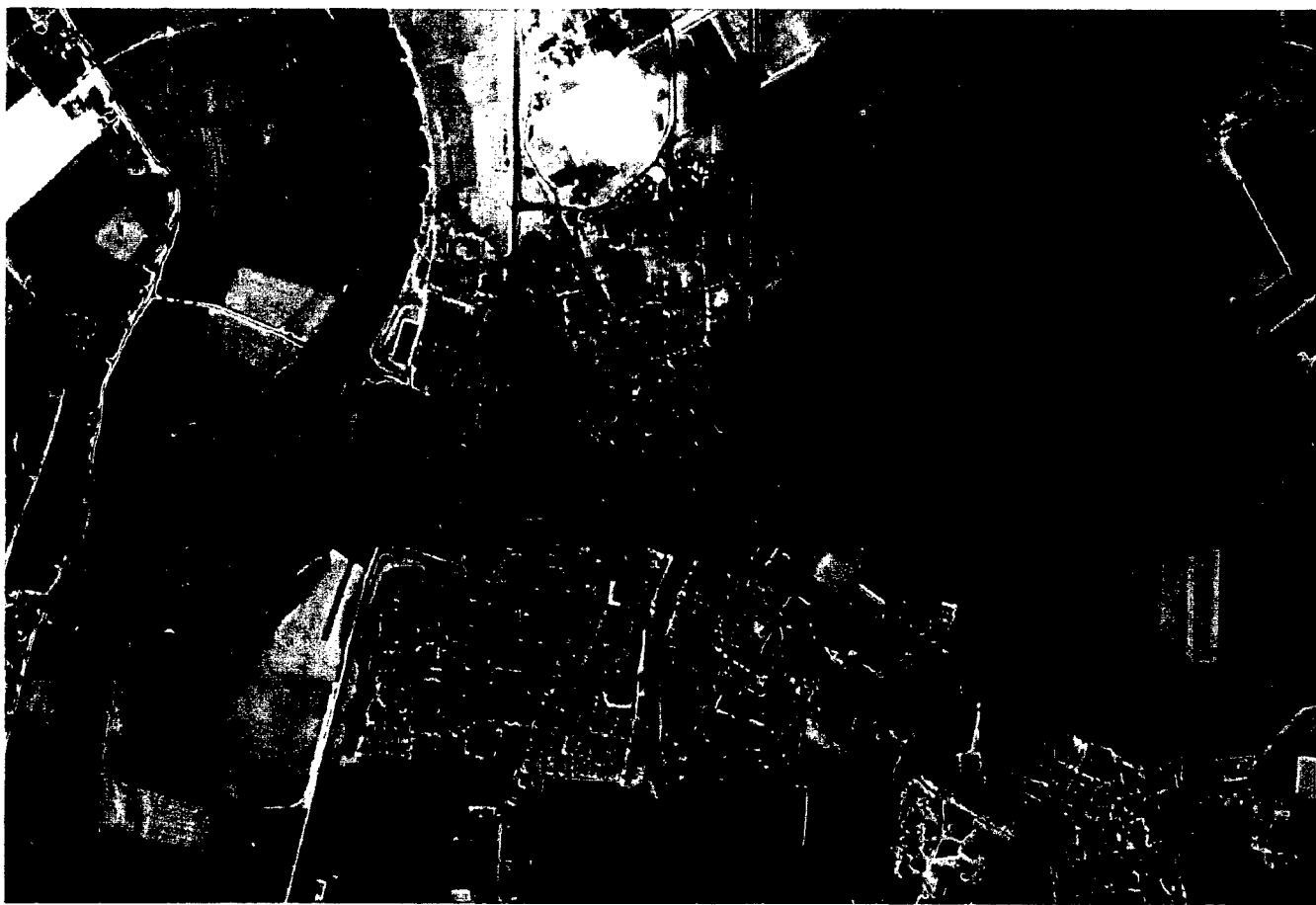


Figure 9: KVR image of the village Olst (bottom) compared with CAESAR image (top). KVR uses the optical window (0.4μ to 0.7μ) with black and white photographic film. Resolution is about 2 m. See for explanation of the CAESAR image Fig. 7.

TIR

The TIR image (Fig. 10, bottom) of Olst was recorded on a clear morning, when the sun was already heating the roofs for some time. The TIR image clearly shows man-made objects like houses in Olst. Note that especially the roofs oriented to the south are heated by the sun and appear white in the image, while the roofs oriented to the north are in the shadow and cool. These appear black in the images.

Vegetation like trees try to regulate their temperature by evaporating plant moisture staying relatively cool therefore, so that they appear black in the image. Water and grassland are greyish since their temperature is intermediate. Bare soil fields heated by the solar radiation become warm, so that they appear bright (see bright field in upper right corner). In the CAESAR image, which is recorded in the same weeks this field colours bluish which is in agreement with the fact that this field is not vegetated (bare soil).



Figure 10: TIR image of village Olst (bottom) compared with PHARUS image (top). The TIR image is recorded in the thermal infrared window (8 -12 μ) and the resolution is 5 meter.

2.3 Freiburg test site

The second test site comprises an area of 52 by 56 km centred on the city of Freiburg in the southern part of Germany. The location is given by UTM co-ordinates (E,N, zone 32) 389000, 5287000 (south west corner) and (E,N, zone 32) 441000, 5343000 (north eastern corner). The site comprises part of the Rhine Valley and a part of the Black Forest, so that a variety of landscapes, like forest and infrastructure is combined with moderate relief. For this test site only satellite remote sensing data are available. One of the main goals for this test site is to study the influence of relief on geographical information extraction and the determination of a digital elevation model with remote sensing.

Table 2: Sensor and image data properties for Freiburg test site.

sensor	platform	resolution (m)	type	date (d-m-y)	time
TM	spaceborne	30	optical/nir	24-06-1994	10:17 (solar)
SPOT XS	spaceborne	20	optical- multispectral	09-05-1989	-
SPOT PAN	spaceborne	10	optical- panchromatic -29.6°	02-07-1994	10:14 (solar)
SPOT PAN	spaceborne	10	optical- panchromatic +00.2°	04-08-1994	10:37 (solar)
SPOT PAN	spaceborne	10	optical- panchromatic -25.5°	06-08-1991	10:18 (solar)
KVR1000	spaceborne	2	optical- photographic	21-05-1992	-
ERS-1	spaceborne	25 (3 looks)	microwave- C-band/VV/23 °	28-06-1994	-
JERS-1	spaceborne	25 (3 looks)	microwave- L-band/HH/35 °	22-04-1994	-

For the registration we collected topographical maps from “das Deutsche Militarische Geowesen”, scale 1:50,000. The following maps with codes: L7510, L7512, L7514, L7710, L7712, L7714, L7716, L7910, L7912, L7914, L7916, L8110, L8112, L8114, L8116, L8310, L8312, L8314, L8316 were available. The registration accuracy of the TM, SPOT and KVR data is comparable to the data of the Heerde test area. An exception are the SPOT oblique images and the ERS and JERS images. Registration of these images involves the use of a DEM, which is therefore somewhat less accurate (see remarks below).

2.4 Description of the Freiburg data

In Figure 11 we show an overview map of the test area (from General Karte no. 24, scale 1:200.000). To the west of the city Freiburg, the Rhine and the Rhine Valley are included. To the East of Freiburg the Black Forest is present including the highest peak (Feldberg, 1493 m). The Rhine Valley is an agricultural area including many lines of transportation, like (rail-)roads and waterways. The Black Forest is covered with forest with in the valley agricultural fields and villages. In Figure 12 we compare the map with a colour coded DEM (DTED). From these maps we see that in the test area we can find flat areas near the river Rhine (altitude 175-200 m above sea level), low level relief (Kaiserstuhl, altitude about

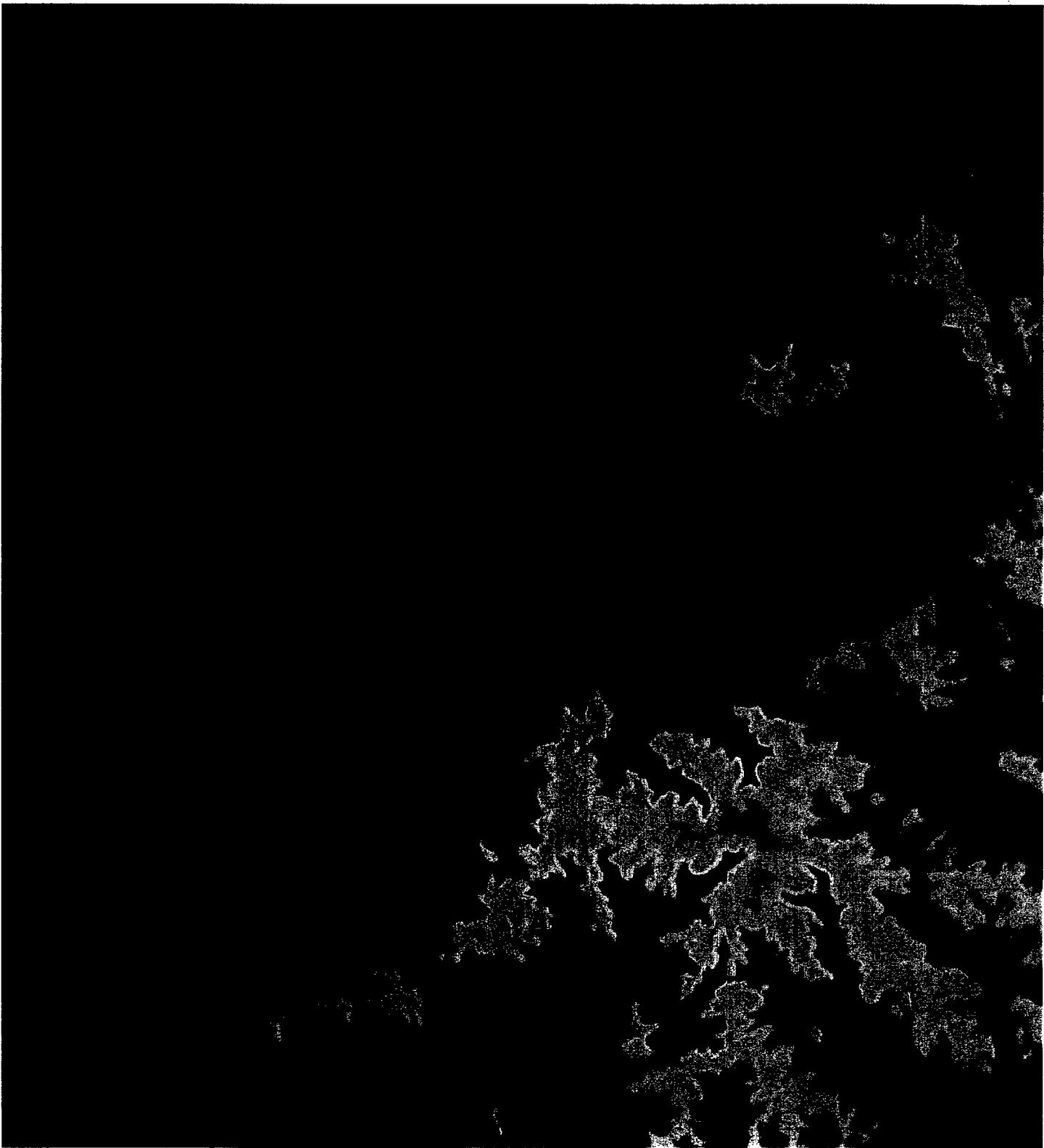
500 m above sea level, north-west of Freiburg) and moderate relief of the Black Forest (altitude from 500 to 1500 m above sea level).

In order to present the higher resolution KVR data we have defined two sub-areas within the test site. One of 10 by 10 km and one of 2 by 2 km centred on Freiburg. The co-ordinates for these areas are 411000, 5314000 (South-west) and 421000, 5324000 (North-east), and 414000, 5315000 (South-west) and 416000, 5317000 (North-east), respectively. For the first we show a part of the 1:50,000 topographical maps (L7912/L8112, see Fig. 16).

The general description of the data is the same as for the Heerde area of course. We will here focus on the influence of the relief which is absent in the Heerde area.



Figure 11: Map of test site Freiburg (from General Karte no. 24, scale 1:200,000). The top is to the North as usual and the dimensions are 52 by 56 Km. Actual scale on paper is 1:275,000.



Height (m)




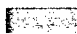
















	175		300		600		1100
	200		350		700		1200
	225		400		800		1300
	250		450		900		1400
	275		500		1000		1500

Figure 12: Digital terrain elevation data (DTED) of test site Freiburg. Ground resolution is 100 by 100 m. Height is colour coded (see legend).

TM

Like for the Heerde test area we show in Fig. 13 band 5, 4 and 3 in the red, green and blue channel respectively. Bare soil and cities colour purple, while the vegetation shows different tints of the green colour depending on the type of vegetation. Remarkable is the area near the mountain Feldberg which colours blue. This is probably due to the bare soil which consists of minerals like chalk. These minerals absorb near-infrared radiation more effectively than optical radiation. The variations in colour for TM images show that multi-spectral imaging in the optical/near-infrared is quite powerful for determining land cover types. Because TM images are recorded in vertical viewing with a small field of view geometrical distortions are small. Only at the edges corrections are sometimes needed.



Figure 13: TM image of test site Freiburg. Band 5 ($1.6\ \mu$), 4 ($0.8\ \mu$) and 3 ($0.65\ \mu$) are shown in the red, green and blue channel, respectively. Resolution is 30 m.

ERS

Due to the effect of layover, foreshortening and shadowing caused by relief (see section S1.3.2, Technical Supplement) the image (Fig. 14) is distorted at places where significant slopes are present. Because the incidence angle of the ERS is quite small (23 degrees) especially foreshortening and sometimes layover is a problem. For the registration it is therefore necessary to use the DEM in order to correct for the distortion. In the case of layover we see bright areas in the image. These areas become stretched when registered so that the resolution locally becomes worse, which is clearly seen in the bright areas of the image. Due to the correction, the registration accuracy varies from place to place in the image, typically from 25 m to 150 m.

Note that the lake in the South East corner shows a clear patch, where waves generated by wind enhance the backscatter.



Figure 14: ERS image of test site Freiburg. Resolution is 25 m, 3 looks. Wavelength is 5.3 cm (C-band), VV polarised, incidence angle is 23 degrees. The image has been corrected for distortions due to relief.

JERS

Like for the ERS the JERS image also suffers from foreshortening, which has been corrected using the DEM. The distortions and the corrections are smaller because the incidence angle is larger, i.e. about 40 degrees. Because of the larger incidence angle and the longer wavelength the Rhine Valley shows more contrast between villages (white), forest (bright) and agricultural land (black). The registration accuracy is variable ranging from 25 m to 150 m, like for the ERS.

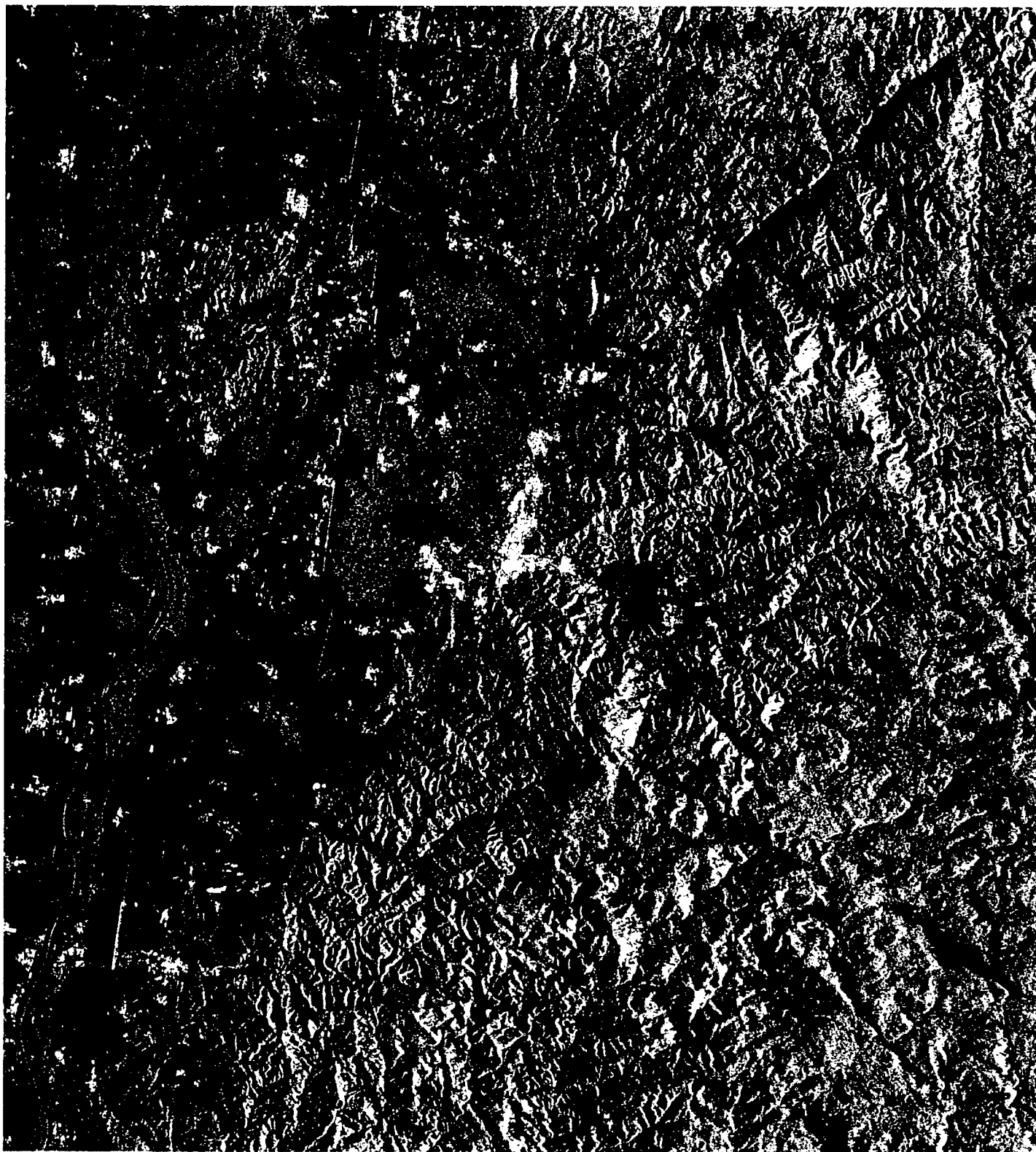


Figure 15: JERS image of test site Freiburg. Resolution is 25 m, 3 looks. Wavelength is 25 cm (L-band), HH polarised, incidence angle is 40 degrees. The image has been corrected for distortions due to relief.

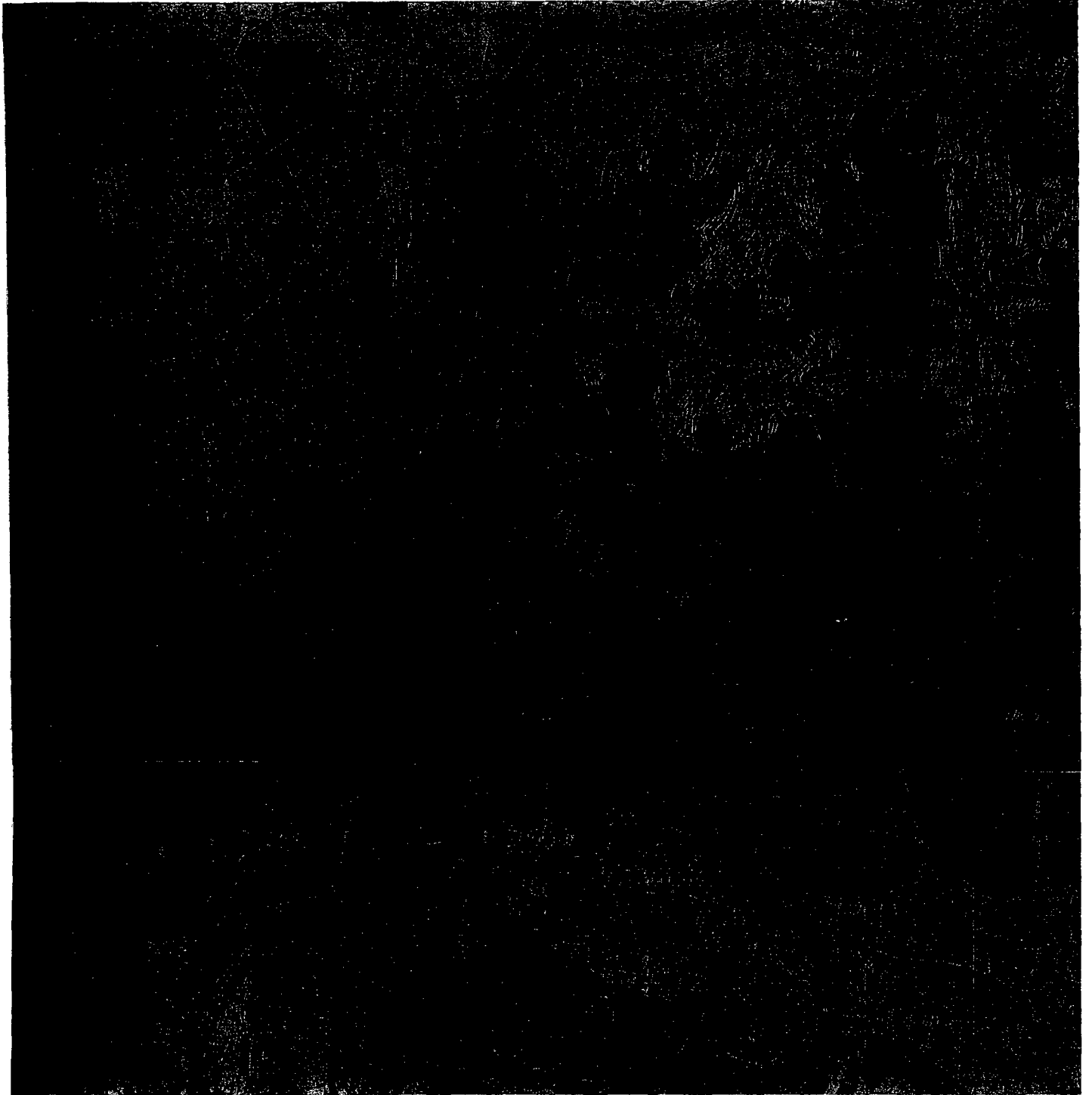


Figure 16: Topographical map 1:50,000 of the city of Freiburg (from *das Deutsche Militärische Geowesen*, map no. L7912 and L8112). The top is to the North as usual and the dimensions are 10 by 10 Km. Actual scale on paper is 1:50,000.

SPOT-PAN and KVR

We compare in Figs. 17, 18, and 19 SPOT and KVR data for the two subareas (see Fig. 16 for a topographical map of the larger sub area). The images from the two sensors agree quite well although they are recorded in different years and seasons. For the SPOT-PAN image we show the one with vertical viewing, so that no distortion due to relief is present, like for the KVR. Quite nicely is visible how details become blurred due to the lower resolution of PAN (10 m) compared to KVR (2m). This is especially apparent in Fig. 19 where KVR also shows the smaller streets, while SPOT only shows the larger roads.



Figure 17: SPOT-PAN image of the city of Freiburg. Optical imaging ($0.5-0.75\ \mu$), resolution is 10 m.

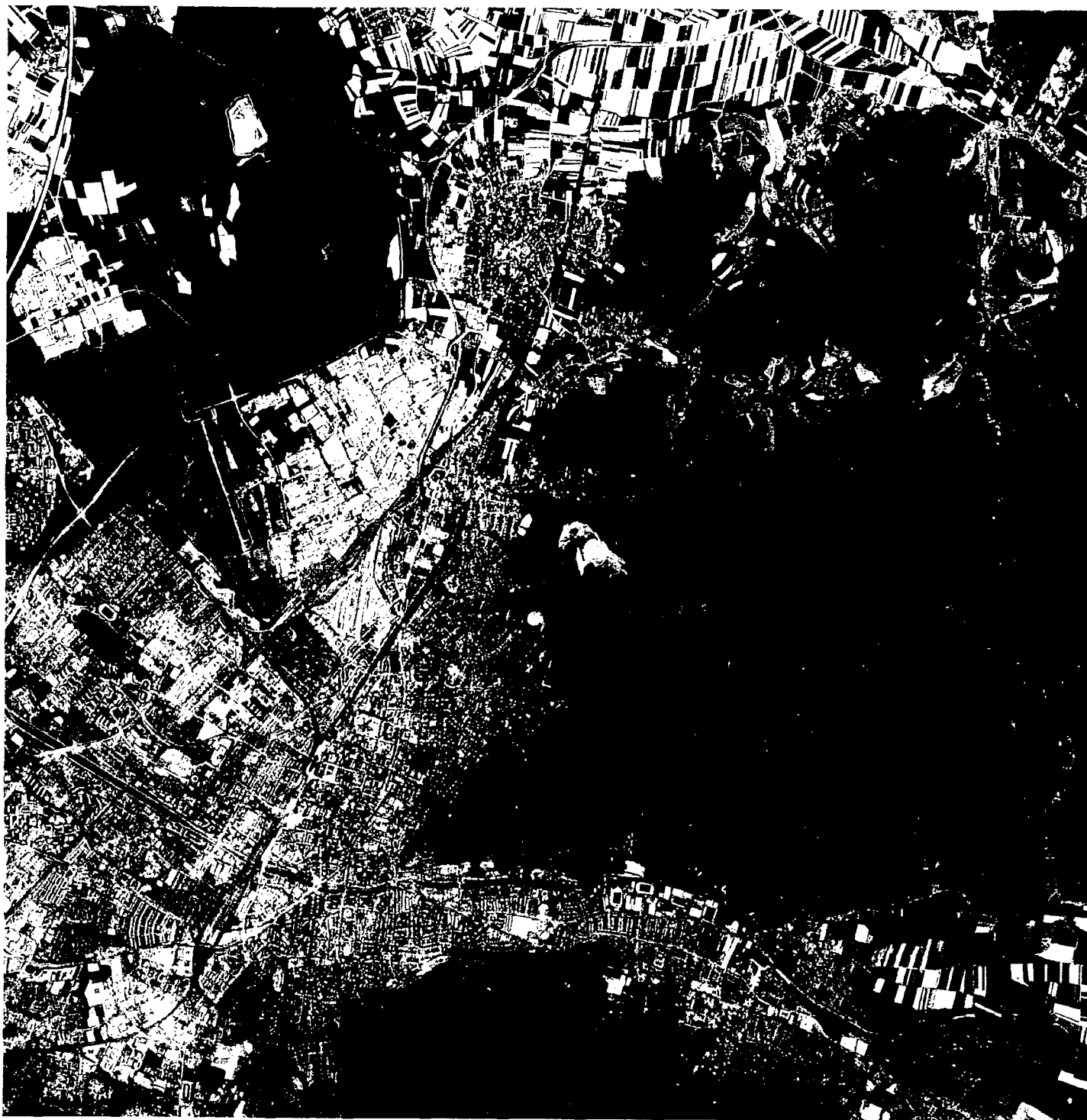


Figure 18: KVR image of the city of Freiburg. Optical photographic imaging ($0.4\text{--}0.7\text{ }\mu$), resolution is 2 m .



KVR



SPOT

Figure 19: KVR image (top) and SPOT-PAN (bottom) image for an area of 2 by 2 km in the city of Freiburg.

3. The ground database (TERAS)

In order to evaluate the remote sensing data for cartographic purposes we have used primarily the so-called TERAS (Terrein analyse systeem) database for the Heerde test site, containing detailed geographical data in vector format. These geographical data are comparable to the information on a topographical map with scale 1:50,000.

At first instance a collection of features and attributes has been selected on basis of their relevance for military terrain inventory. These features and attributes are extracted from a DIGEST (digital geographical information exchange standard) code list. About 60 features have been selected covering 6 categories, which are listed here:

1. Culture; which includes typically man-made object like buildings, roads etc. (code A).
2. Hydrography; for example rivers, canals, ditches, lakes etc. (code B)
3. Relief portrayal; spot elevation, contour lines (code C)
4. Land forms; for example barren ground, depression (code D)
5. Vegetation; for example trees, crop land (code E)
6. Demarcation; e. g. an administrative boundary (code F)

The complete list of features with their DIGEST coding is shown in Table 3. Not for all features vector data are available in the TERAS database. In Table A1 of the Appendix we have listed for which features in Table 3 vector data are available and for which are not. Also shown in Table A1 of the Appendix are features not included in Table 3, but for which data are available in the TERAS database.

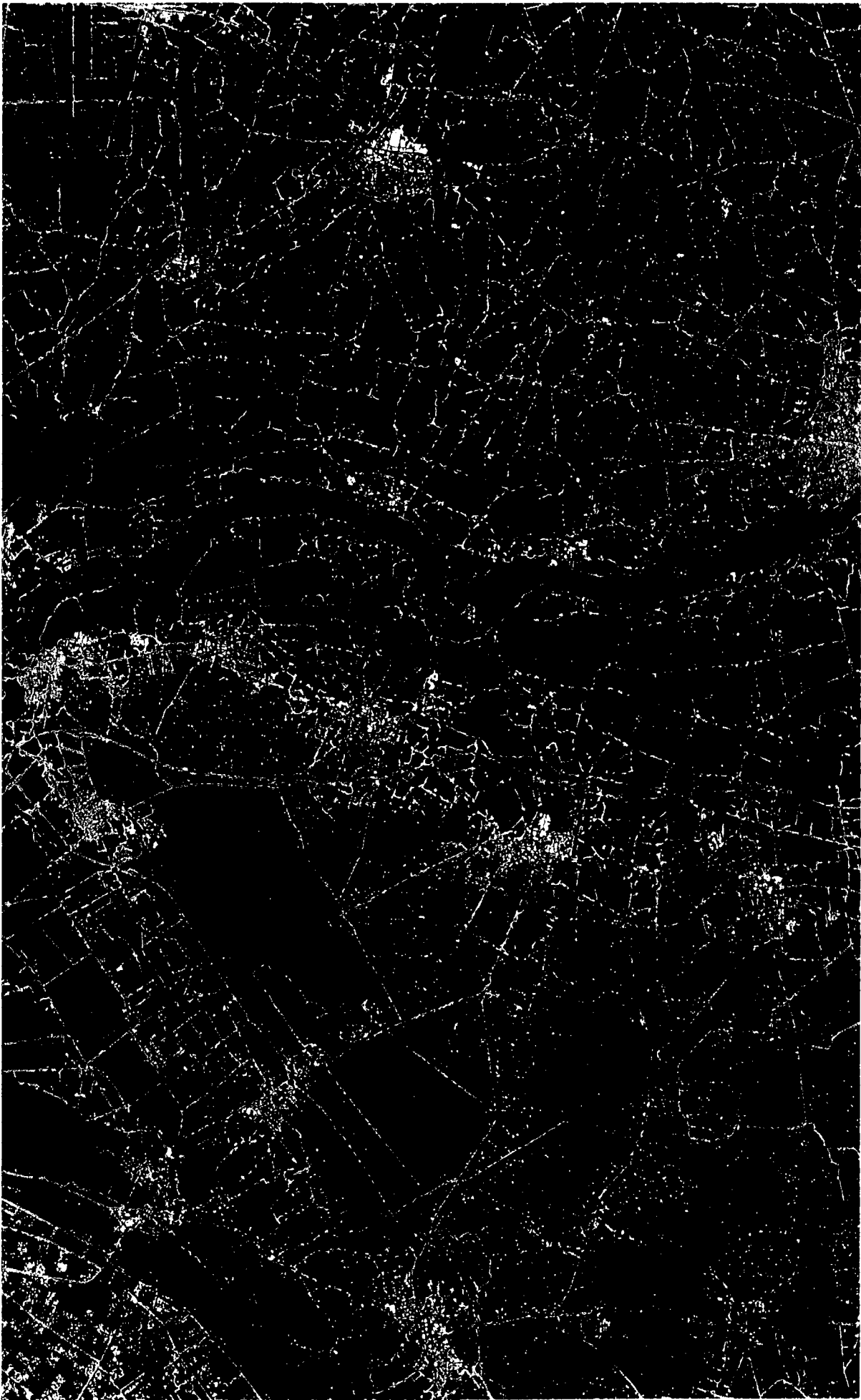


Figure 20: Two features of the TERAS database are shown as an overlay on top of the ERS image. The roads (AP030) are shown as yellow lines, while the buildings (isolated) are shown as red dots.

As is usual for vector data, they can appear in three formats: points, lines and polygons. The data for a feature usually consists of one format depending on what is appropriate. For example, towers are points, roads are lines and crop lands are polygons. In some cases (e.g. AL020) point, line as well as polygon data are available.

To give an impression of the data we show in Figure 20 the roads (AP030, lines) and isolated buildings (AL020, points) which are contained in the TERAS database as an overlay on ERS data. Note that the database for these features is rather complete except in the build-up areas where only the main roads are included in the database and no isolated buildings are present. Also note that most buildings are near a road, which can be expected of course.

Features can be accompanied by attributes, which give information about the features like, for example, the width of roads and which are usually presented in the form of a Table. In advanced GIS systems this information can also be shown on a display.

Table 3. List of features and attributes.

Feature		Attribute	
ID	name	ID	description
Culture			
AD010	Power plant	HGT LEN	height above surface level length or diameter
AD030	Substation		
AJ050	Windmill	HGT	height above surface level
AL015	Building	BFC HGT	building function category height above surface level
AL020	Built-up area	HGT PPT	height above surface level populated place type
AL070	Fence	FTI	fence type indicator
AL260	Wall	HGT	height above surface level
AL240	Tower	HGT	height above surface level
AF010	Chimney		
AF030	Cooling Tower		
AF040	Crane		
AF070	Flare Pipe		
AT080	Commun. Tower		
AM280	Water Tower	CAP HGT	capacity height above surface level
AN010	Railroad	LTN RRA RRC	track/lane number railroad power source railroad categories

AP020	Interchange	LC1 LC2 LC3 LC4	load class type 1 load class type 2 load class type 3 load class type 4
AP030	Road	LC1 LC2 LC3 LC4 OHC RST SGC	load class type 1 load class type 2 load class type 3 load class type 4 overhead clearance category road/runway surface type slope/gradient
AQ040	Bridge	LC1 LC2 LC3 LC4 NOS	load class type 1 load class type 2 load class type 3 load class type 4 number of spans
AQ045	Bridge Span	LC1 LC2 LC3 LC4 EXS	load class type 1 load class type 2 load class type 3 load class type 4 existence category
AQ065	Culvert		
AQ116	Pumping Station		
AQ135	Vehicle Stop. Area	SWL	single wheel bearing load
AT030	Power Trans. line		
AT040	Power Trans. pylon		

Hydrography

BB140	Jetty		
BG010	Current flow		
BH020	Canal	WDA WID	water depth average width
BH030	Ditch	WID	width
BH080	Lake/pond	SCC	spring/well characteristic category
BH090	Inundation		
BH100	Moat	WID	width
BH115	Underground water		
BH140	River/stream	DOF WID WVA	direction of flow width water velocity average
BH501	Waterway		
BI020	Dam/Weir	EXS	existence category
BI040	Sluice Gate	MCC	material composition category
BI030	Lock		

Relief Portrayal

CA030	Spot Elevation	ZV1	lowest Z value
CA010	Contour line		

Land forms

DA010	Ground Surf. Elem.	STP SWC	soil type soil wetness condition
DA020	Barren Ground		
DB070	Cut		
DB080	Depression	ZV1	lowest Z value
DB090	Embankment	HGT MCC	height above surface level material composition category
DB501	Upper Part of Cliff		
DB010	Cliff		

Vegetation

EA010	Cropland		
EA020	Hedgerow		
EA040	Orchard/Plantage		
EB020	Scrub/Brush	DMT PHT	density measure predominant height
EC030	Trees	DMT HGT SDS TSC VEG	density measure height above surface level stem diameter size tree spacing category vegetation characteristics

Demarcation

FA000	Admin. Boundary	USE	usage
FA001	Admin. Area		
FA015	Firing Range		
FA165	Training Area		

The attribute data in the TERAS data-set is quite limited and not easy to handle in the vector module of the image processing system ERDAS (see Appendix). We have decided therefore to restrict the comparison to the features only. The attributes are considered globally in the Table A7 of the Appendix and in the Image Catalogue.

Due to several conversions from the original DIGEST A format to generic ArcInfo format within the TERAS database the polygon data have been corrupted. No real polygons could therefore be constructed. Only the contours of the polygons could be inspected after a correction. To support the comparison also a digital and co-registered scanned version of the topographical map 27 (1:50,000) has been used.

Not all features in the list of Table 3 are suitable for comparison. For example contour lines, administrative boundaries etc. are difficult to monitor with the current remote sensing data or are absent in the Heerde test area. We divided the list of Table 3 in two lists, one suitable for comparison and one not suitable for comparison (see Table A2 of the Appendix).

To distinguish between related features (for example the group of tower-like features) one need to identify these features. A first inspection of the available data-set showed that this is not possible and that we have to restrict ourselves to detection and recognition in this study. Identification would require sub-meter resolutions not present in this data-set. Since it is not useful to compare different features which cannot be separated in the remote sensing images, we grouped together several features for comparison (see Table A2 of the Appendix).

Therefore no distinction is made between the different towers. Also all buildings/complexes are considered as one feature in the comparison. Taking the features suitable for comparison and grouping the features together, only three categories (Culture, Hydrography and Land forms/vegetation) are left. In order to avoid confusion we have assigned an alternative code to the new features in this compressed list, where the second letter of the code is 'p', 'l' or 'a' indicating whether the feature is a point, line or area (polygon), respectively. This list shown in Table 3b.

Table 3b. Compressed list of features used in the comparison with remote sensing data.

Culture		Hydrography		Land forms/ vegetation	
Ap1	bridge	Bp1	lock/weir	Ea1	barren ground
Ap2	culvert	B11	jetty	Ea2	cropland
Ap3	stopping area	B12	canal	Ea3	heath
Ap4	tower	B13	dam	Ea4	hedge row
Ap5	building/com plex	Ba1	lake/ponds	Ea5	orchard
Ap6	pylon	Ba2	inundation	Ea6	trees
Al1	fence				
Al2	railroad				
Ap9	road				
Al4	high tension line				
Aa1	substation				
Aa2	build-up area				

4. Comparison of the ground database with the remote sensing data-set

4.1 Introduction

In this section we present the results of the comparison between vector data available in the TERAS data-set and remote sensing data collected for this study. The purpose of this comparison is to evaluate how accurately geographical information can be extracted from remote sensing sensors assuming that the TERAS data-set can be used as a complete reference data-set. In this way we try to determine the potential of remote sensing data for geographical information extraction.

4.2 The remote sensing data used

In the comparison we have used the remote sensing images of the Heerde test area. For the satellite images we used TM, Spot-PAN and KVR. The Spot-XS image has been omitted in the comparison since it is expected that the results will average the results of PAN and TM. Also the ERS and JERS images are not considered here since the results are expected to be marginal compared to the other sensors. Only extracted point targets from these images have been compared with point features in the TERAS data-base. These results are shown and discussed in section 4.4 and 4.5. For the airborne images we used CAESAR 3 m data, the PHARS data and TIR data.

4.3 Method of comparison

By comparing the various remote sensing images with the TERAS data-set (if needed also with the digitised topographical map) we have tried to determine for every feature how much of a feature was seen (i.e. *detected*) in the image. To do this different methods had to be used. For point data it is possible to count the number of points which are clearly related to objects seen in remote sensing images. The number of points which can be evaluated varies a lot for the different features. Usually the whole "Heerde" test area as imaged by PHARS and CAESAR has been taken for evaluation. In some cases the number of points is very large and a smaller area has been taken. In case of line or polygon objects also the length and area plays a role. A result is then obtained by inspection, for example by estimating the total detected length or area. Areas and methods used are summarised in Table A8-A11 of the Appendix.

4.4 Results of the comparison

The results of the comparison are summarised in Table 4 for the six sensors covering three wavelength regions and resolutions ranging from 30 to 2 meter. The results are shown for the three classes: Culture, Hydrography and Land forms/Vegetation. We discuss here the results for the three classes separately.

Culture

Some features like 'fences', 'towers' and high tension lines are generally too small to be detected by the sensors. For the detection of these features resolutions of less than 1 meter are required which are not available in the data-set. The low success rate of detection of towers is explained by the fact that towers are small when they are observed in vertical direction. For microwave sensors the viewing or look direction is not vertical (slant range geometry). The detection of towers is hindered in this case since the targets are confused with other targets in build-up areas where most of the towers are located.

The resolution of the TM sensors (30 m) causes this sensor to be less effective for detecting features in the category 'culture'. For SPOT-PAN the resolution of 10 meter makes this sensor 'intermediately' successful.

Because KVR and CAESAR have relatively high resolutions (2-3 meter) most of the features are detected. Despite the somewhat lower resolution of CAESAR (3 m) compared to KVR (2 m) the first has a slightly higher success rate than the second because of the spectral information. Due to this information man-made objects and vegetation are easier to discriminate.

The results for the TIR data are very sensitive to the emission and therefore to the temperature of the objects. The TIR data used here have been recorded during quite optimal conditions (late morning, clear sky). Man-made objects like bridges, roads and especially buildings are detected quite successfully, since they have been heated by solar radiation.

For the PHARS sensor the smaller objects like culverts and the smaller roads are difficult to detect because of the relatively low resolution (6 m) combined with the speckle (see also section S1.3.1 of the Technical Supplement).

Hydrography

The dimension of lakes and canals can vary substantially. For example the feature 'lakes' in the TERAS data-base contains many ponds sometimes overgrown by trees and the feature 'canals' contains many small ditches. This causes the detection rate to be quite low for the lower resolution sensors (TM and SPOT-PAN) despite the fact that these features are generally easy to detect.

The feature 'inundation' (IJssel Uiterwaarden) is difficult to observe directly since its main property is small scale relief over a large area. However the land use is different for the inundation compared to the surroundings so that observation of the land use makes detection indirectly possible. It appears that high resolution (< 5 meter) is advantageous for this purpose.

The discrimination between water and vegetation is clearly more difficult for PAN recordings (SPOT, KVR) compared to multi-spectral recordings (CAESAR). For the PHARS sensor the detection of canals is hindered by confusion with roads. Despite the relatively high resolution of the TIR sensor (5 meter) the detection rate is substantially lower than that for the other high resolution systems (KVR, CAESAR) due to the fact that the contrast between water and the surroundings is not very high, especially when the water is surrounded by vegetation. However it should be noted that under certain circumstances (e.g. relatively warm water on a cold night) water can be a dominant feature in the image.

Land forms/vegetation

In this case resolution is a less crucial parameter, since most objects are extended. For detection other information is important. Especially multi-spectral information plays a dominant role. This is due to the fact that vegetation reflects most of the light in the near-infrared compared to other (e.g. man-made) objects.

By observing in the near-infrared vegetation differences also become apparent. It is therefore that the TM sensor has an even higher detection rate compared to the Spot-PAN sensor despite the difference in resolution. The same is true for the CAESAR compared to the KVR sensor.

The detection rate of the PHARS sensors is lower on average compared to the multi-spectral optical sensors. Like in the optical, also in the microwave wavelength region vegetation differences are more easily observed when additional information is available, for example from multi-wavelength systems or polarimetric systems. The single channel PHARS sensor therefore shows a relatively low detection rate.

The TIR sensor is not ideal for discrimination between different types of vegetation, since vegetation attempts to suppress temperature differences by controlling the evaporation of plant moisture. The detection rate is consequently relatively low.

Table 4. Summary of the ability to detect features for the different sensors

	Name	TM	PAN	KVR	CAESAR	PHARS	TIR
--	------	----	-----	-----	--------	-------	-----

Results for category culture

Ap1	bridge	10%	50%	80%	> 90%	50%	90%
Ap2	culvert	< 10%	20%	70%	80%	20%	20%
Ap3	stopping area	0%	30%	90%	90%	10%	50%
Ap4	tower	< 10%	< 10%	10%	10%	< 10%	< 10%
Ap5	building/com plex	50%	90%	100%	> 90%	80%	100%
Ap6	pylon	< 10%	10%	70%	90%	90%	< 10%
Al1	fence	0%	0%	< 10%	< 10%	0%	0%
Al2	railroad	70%	90%	100%	100%	100%	80%
Ap9	road	20%	70%	> 90%	100%	50%	70%
Al4	high tension line	0%	0%	0%	0%	< 10%	0%
Aa1	substation	< 10%	60%	90%	90%	90%	90%
Aa2	build-up area	60%	80%	> 90%	100%	> 90%	100%

Culture	Average	21%	43%	67%	71%	50%	52%
---------	---------	-----	-----	-----	-----	-----	-----

Results for category hydrography

Bp1	lock/weir	0%	0%	30%	40%	40%	40%
Bl1	jetty	< 10%	40%	90%	> 90%	> 90%	50%
Bl2	canal	30%	20%	60%	80%	30%	50%
Bl3	dam	20%	40%	50%	40%	40%	30%
Ba1	lake/ponds	30%	30%	60%	80%	80%	50%
Ba2	inundation	0%	30%	50%	50%	30%	50%

Hydrography	Average	15%	27%	57%	63%	52%	45%
-------------	---------	-----	-----	-----	-----	-----	-----

Results for category land forms/vegetation

Ea1	barren ground	90%	70%	70%	100%	20%	20%
Ea2	cropland	60%	60%	70%	90%	80%	70%
Ea3	heath	70%	80%	80%	80%	50%	40%
Ea4	hedge row	50%	70%	80%	90%	80%	90%
Ea5	orchard	70%	10%	50%	50%	20%	< 10%
Ea6	trees	60%	80%	90%	100%	90%	100%

Land forms/ Vegetation	Average	67%	62%	73%	85%	57%	55%
---------------------------	---------	-----	-----	-----	-----	-----	-----

4.5 Other comparisons with remote sensing data

Roads

By displaying the remote sensing images on screen and digitising the detected roads (AP030) manually a database was created containing vector data for the different remote sensing sensors for the Heerde test area. The total length of the roads can be calculated and compared with the total length of the roads in the TERAS database. In this way a more quantitative comparison can be obtained compared with the inspection method discussed above. We show the total length (in meters) and some statistics in Table 5.

Table 5. Statistical data for AP030.

<i>Database</i>	<i>no. of elem.</i>	<i>total length (m)</i>	<i>mean length (m)</i>	<i>s.d. length (m)</i>
TERAS	1646	433695	263	242
TM	1	107505	-	-
PAN	169	311750	1845	1621
KVR	2536	453285	178	201
CAESAR	807	619553	768	1256
PHARS I	64	147523	2305	2876
PHARS II	311	417945	1344	1638
TOP50	702	557823	774	1337

The total length indicates how well roads can be extracted from the images. Most images do not show as many roads as are present on the topographical map. Only the CAESAR scanner shows even more roads since also unpaved roads are seen. Note that for PHARS two entries are available in Table 5. For PHARS I only the more obvious cases (dark lines) are extracted as roads. For PHARS II less restrictions are made and most of the dark lines are extracted as roads. Since roads (AP030) and canals (BH020) are easily confused in microwave images the result will be overestimated.

Point features

Microwave images are suitable for automatic point target extraction. Point targets can give increased backscatter which can easily be discriminated from the background with statistical means. The extracted points can be compared automatically with point features in the TERAS data-base, so that a quantitative comparison is possible. In this way ERS and JERS data, having improperly low resolutions for cartographic applications, may be used for the detection of point features.

The comparison has been made for three ERS and one JERS images (see Table 6) and for the complete area covered by the maps 27 East and 27 West. A point was extracted from the images when the backscatter was 4.3 dB above the background giving more than 99% confidence that the point is not due to speckle.

Table 6. Comparison results for the ERS/JERS and the TERAS point data-set

Case	Data	Date	Pass	Result
1	ERS 1	23 06 92	ascending	22%
2	ERS 2	02 07 92	descending	20%
3	ERS 3	23 06 92	descending	24%
4	JERS	20 09 93	descending	20%

For the comparison with the TERAS database the following points features in the TERAS data base have been selected: AJ050, AL240, AF010, AF040, AT080, AM280, AL015, AL020, AQ116 and AQ125, giving about 3500 points representing mostly buildings and towers.

A point feature in the TERAS data-set selection was said to be detected when it coincided within 50 m with a point extracted from the RS image. The result is that about 20% of the point features in the TERAS data-base are 'seen' by ERS and JERS (see Table).

Another question is then how many of the 'detected' points are the same for all four cases, since the data not only differ in time but also in azimuth angle (different for descending and ascending passes) and in sensor (ERS/JERS). It appears that for cases 1 and 2 (difference in azimuth angle and time) 40% is the same, while for cases 2 and 3 70% is the same (difference in time only) and for cases 3 and 4 30% is the same (difference in sensor and time). The low value for cases 1 and 2 can be explained by the fact that the backscatter from point targets is quite dependent on the azimuth angle.

4.6 Estimation of the resolution required for obtaining geographical information

In the comparison (see section 4.5) features from the existing database (TERAS, maps) were inspected whether they were 'seen' in the remote sensing images. In this way only the ability for detection could be estimated, but not for recognition. On basis of certain criteria (e.g. feature properties like dimension, shape, appearance, but also context information) we have estimated for every feature, which resolution is at least needed in order to detect and to recognise these features.

The results are presented in Table 7 (column 3 and 4 for detection and recognition, respectively) for the compressed feature list using 6 resolution categories ranging from extremely low (> 50 m) to extremely high (< 1 m). For each feature we have assigned a resolution category with the lowest possible resolution for detection and recognition. Higher resolution also suffices of course, but for lower resolution it is foreseen that detection or recognition, respectively, is not possible anymore. In Figure 21 the categories are statistically analysed. We assume that the resolution categories are valid for all three wavelength regions.

In Table A5 of the Appendix we show the results for every feature of Table 3. The criteria used are listed in Table A6 of the Appendix and are explicitly given per feature for detection and recognition.

The results for detection in Table 7 (column 3) can in principle be compared with the results obtained from the comparison between the remote sensing data-set and the TERAS data-base. In this way the reliability of the results in Table 7 can be tested. We have therefore determined to which resolution category a sensor of our data-set belonged and determined in which resolution category about 50% of a feature was 'seen' (see Table 4). These results are shown in column 5 of Table 7 and should be comparable with column 3. In general the columns match, but there are a few exceptions which we will discuss below.

Table 7. Resolution categories required for detection and recognition.

- + = extremely low (> 50 m)
 ++ = very low (15-50 m)
 +++ = low (8-15 m)
 ++++ = high (3-8 m)
 +++++ = very high (1-3 m)
 ++++++ = extremely high (<1 m)

ID	Feature	Resolution category required for detection (estimated)	Resolution category required for recognition (estimated)	Resolution category required for detection inferred from RS data-set
----	---------	--	--	--

Results for category culture

Ap1	bridge	++++	+++++	+++
Ap2	culvert	+++++	+++++	+++++
Ap3	stopping area	+++	++++	++++
Ap4	tower	++++	+++++	-
Ap5	building/com plex	+++	++++	+++
Ap6	pylon	++++	+++++	++++
Al1	fence	+++++	+++++	-
Al2	railroad	+++	+++++	++
Ap9	road	+++	++++	+++
Al4	high tension line	+++++	+++++	-
Aa1	substation	+++	+++++	+++
Aa2	build-up area	+	++	++

Results for category hydrography

Bp1	lock/weir	++++	+++++	+++++
Bl1	jetty	+++	++++	+++
Bl2	canal	++	+++	++++
Bl3	dam	++++	+++++	+++++
Ba1	lake/ponds	++	+++	++++
Ba2	inundation	-	-	+++++

Results for category land forms/vegetation

Ea1	barren ground	+++	+++	+++
Ea2	cropland	++	+++	++
Ea3	heath	++	++++	++
Ea4	hedge row	++++	+++++	+++
Ea5	orchard	++	++++	-
Ea6	trees	++	++++	++

We discuss here the features for which columns 1 and 3 deviate significantly. This is the case for features Ap4 (tower), Al1 (fence), Al4 (high tension line), Bl2 (canal), Ba1 (lake/ponds), Ba2 (inundation) and Ea5 (orchard).

- AP4 (tower). In Table 4 (column 5) only low values for the detection of towers are found. Main problem for the optical and thermal infrared sensors is that the viewing direction is vertical. In that case towers appear as small objects which are not easily detected. When the viewing direction would be oblique the vertical appearance of the tower becomes visible which would facilitate the detection. The results in columns 3 and 4 assume oblique viewing, however. For microwave sensors the look is in range direction (i.e. comparable to oblique viewing) and it is expected that a (point) target will be present in the image due to the scattering mechanism of double bounce refraction. Because most towers in the TERAS data-set are found in build-up areas the targets were easily confused with many other targets hindering the detection.
- Al1 (fence). In the comparison between the remote sensing data-set with the TERAS data-set the available fences could not be seen directly, since they were too small to be detected with resolutions not better than a few meter. Detection therefore requires resolutions of 1 meter or smaller.
- Al4 (high tension line). High tension lines are so small that they hardly can be detected directly. Only in special circumstances in microwave images they can be seen.
- Bl2 (canal). In the comparison of the remote sensing data-set with the TERAS data-set many ditches are present, so that for detection a fairly high resolution category is found in column 3. The estimate for column 1 was done with somewhat larger and broader canals in mind.
- Ba1 (lake/ponds). In the comparison of the remote sensing data-set with the TERAS data-set many small ponds were present, so that for detection a fairly high resolution category is found in column 3. The estimate for column 1 was done with somewhat larger lakes in mind.
- Ba2 (inundation). Inundation could be detected in the comparison of remote sensing data-set with the TERAS data-set because the 'IJssel Uiterwaarden' showed a different land use compared to the surrounding land. Detection is in this case only indirect. For column 1 we assessed direct detection and concluded that detection is not possible.
- Ea5 (orchard). It appears that for the detection of orchards spectral information is important (see results for TM in Table 4), so the determination of the resolution dimension in column 1 and 2 is only valid when enough other information (spectral information) is available.

Below we show a histogram with the number of features as a function of the resolution categories for detection and recognition. From this histogram some average information can be obtained. For example it is clear from the histogram that to detect geographical features in most cases category '++++' (3-8 m) suffices, while for recognition a significant fraction of the features requires resolution

categories '+++++' (1-3 m) and '++++++' (< 1 m). We conclude therefore that in general most geographical information can be detected with sensors having a resolution of 5 meter or less. In order to be able to recognise geographical information resolutions of 1 meter or less are needed. Of course these are averages and as is discussed above also other properties of sensors play a role.

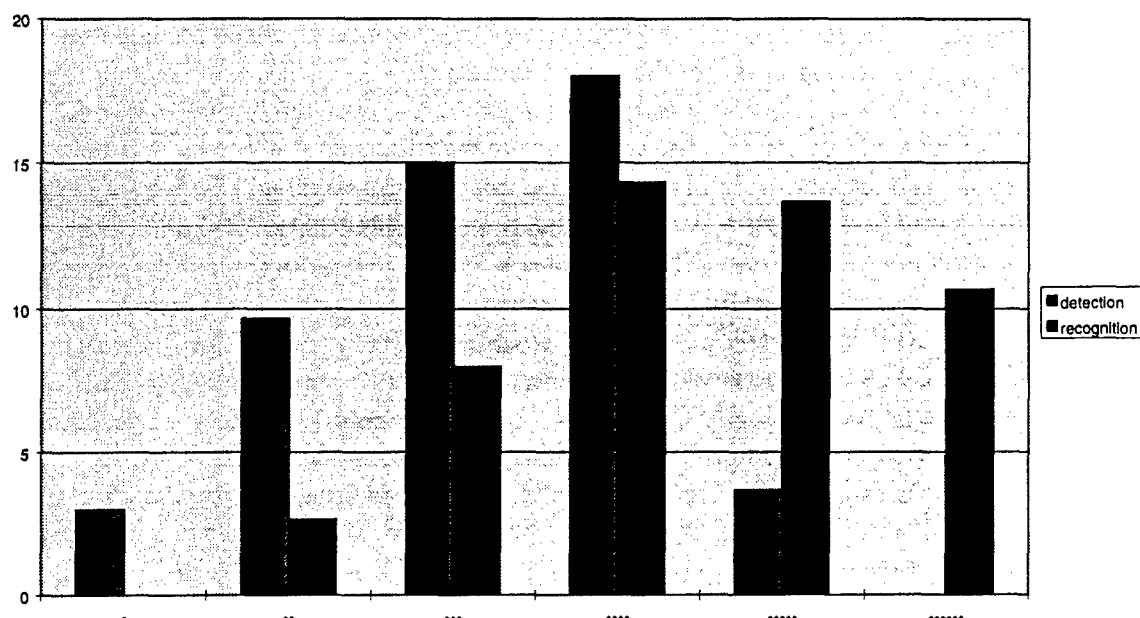


Figure 21: Histogram showing the number of features from Table 3 as function of the resolution categories for detection and recognition.

5. Relief

5.1 Influence of relief on remote sensing images

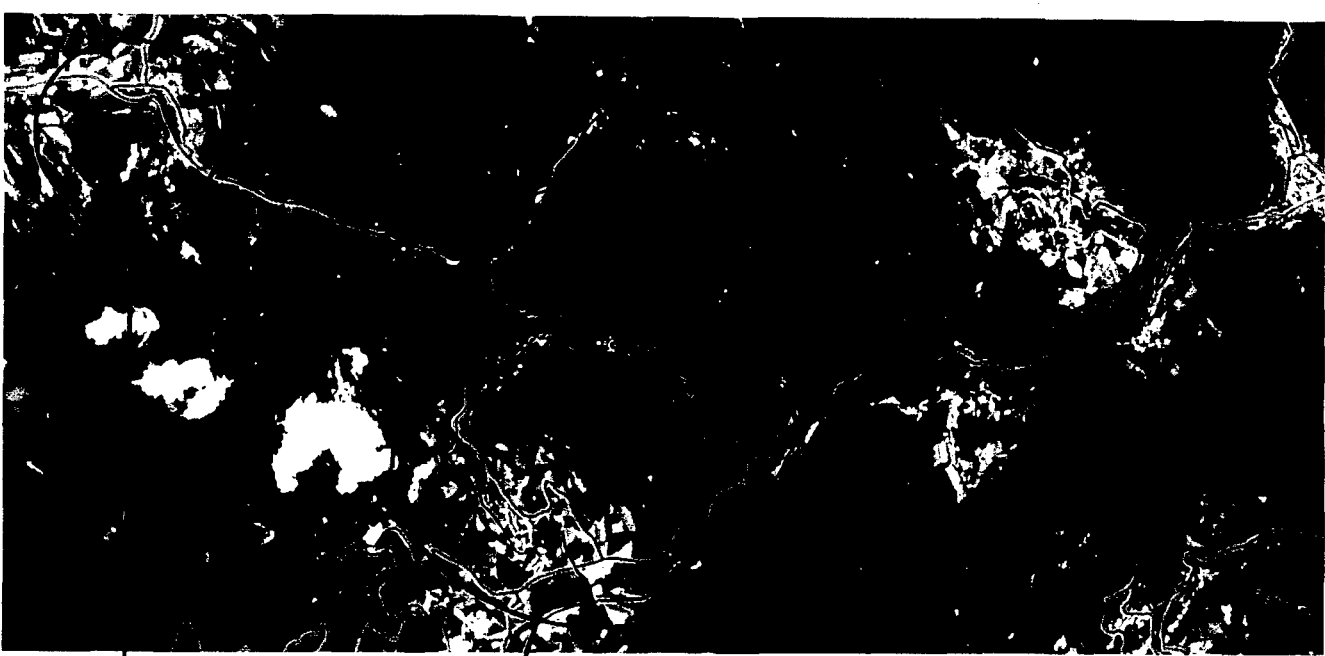
Relief will influence remote sensing images. This means that with respect to a topographical map geometrical distortions occur when the viewing direction is not vertical for optical and thermal infrared imagery and not horizontal for microwave imagery. Even for optical imagery with vertical viewing the viewing direction at the edges is never perfectly vertical. This means that also distortions at the edges occur, which are significant when the field of view is relatively large. Since microwave sensors are always side-looking relief distortions are always present. In the following we show two examples, one for SPOT-PAN and one for the ERS satellite.

Optical

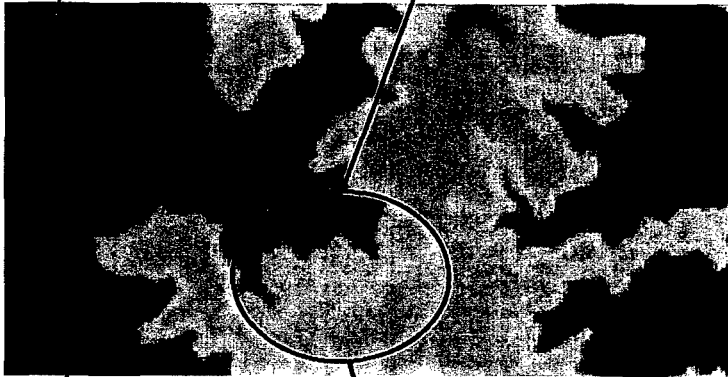
When optical images are recorded with oblique viewing relief will cause geometrical distortions (see section S1.1.2 of the Technical Supplement). An example of distortion due to relief is presented in Figure 22 for SPOT-PAN. Two SPOT-PAN images are shown for a mountainous part of the Black Forest (test site Freiburg). One image is made with vertical viewing while the other used an oblique viewing direction. The images are co-registered using ground control point in the dales. The roads (yellow lines, see Fig. 22) in the dale are correctly registered in both images. For the higher area the yellow lines only agree with the roads in the image with vertical viewing, while they are displaced from the roads in the image with oblique viewing (green lines versus yellow lines). Identifying these displacements is the basis for height information extraction and the generation of a DEM.

Microwave

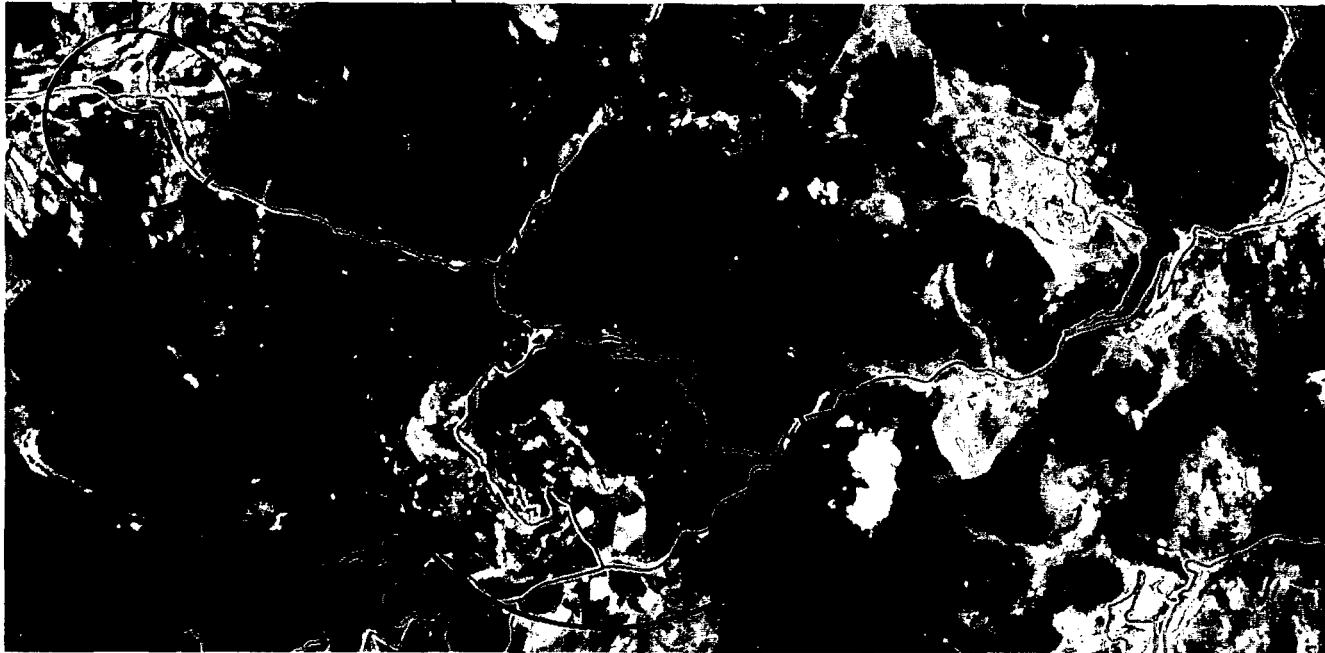
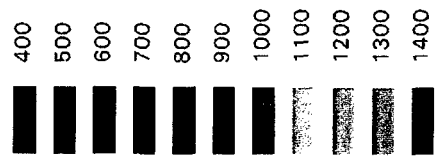
Microwave images of areas with relief suffer both from geometrical and radiometric distortions. There are 4 types of distortions, called foreshortening, darkening, lay over and shadowing. The latter two are anomalies where information is really lost. We present here an example of ERS data for the Freiburg test area in Figure 22. The Figure shows in the left panel the image not corrected for relief, while in the right panel the corrected image is seen. Which distortion occurs depends on the look angle and the local slope angles. Since the look angle of the ERS is rather small mainly foreshortening and lay over occurs. These are visible in the image as the bright areas. Clearly is seen that the resolution is poor in these bright areas. For more information about geometrical distortions we refer to section S1.3.2 of the Technical Supplement.



Spot-PAN oblique

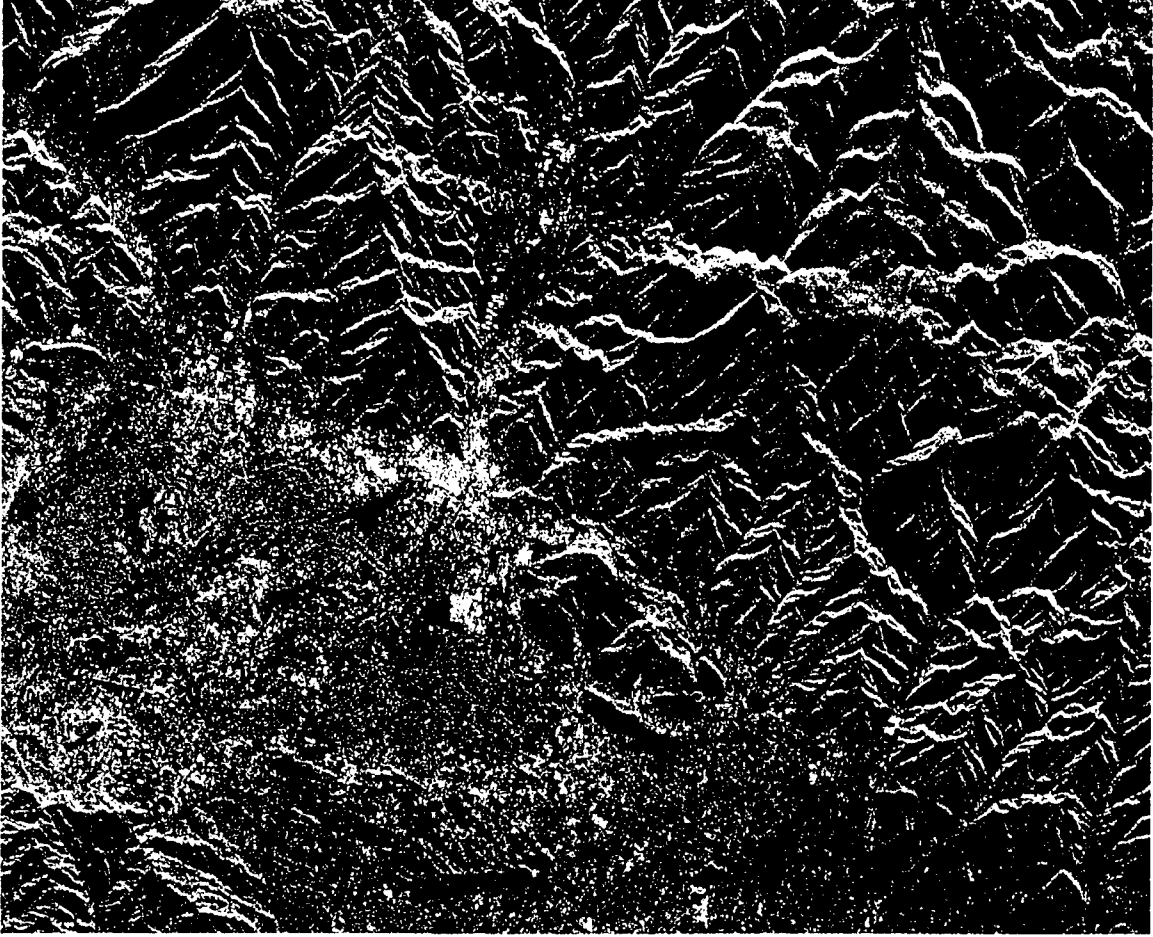


Height (m)

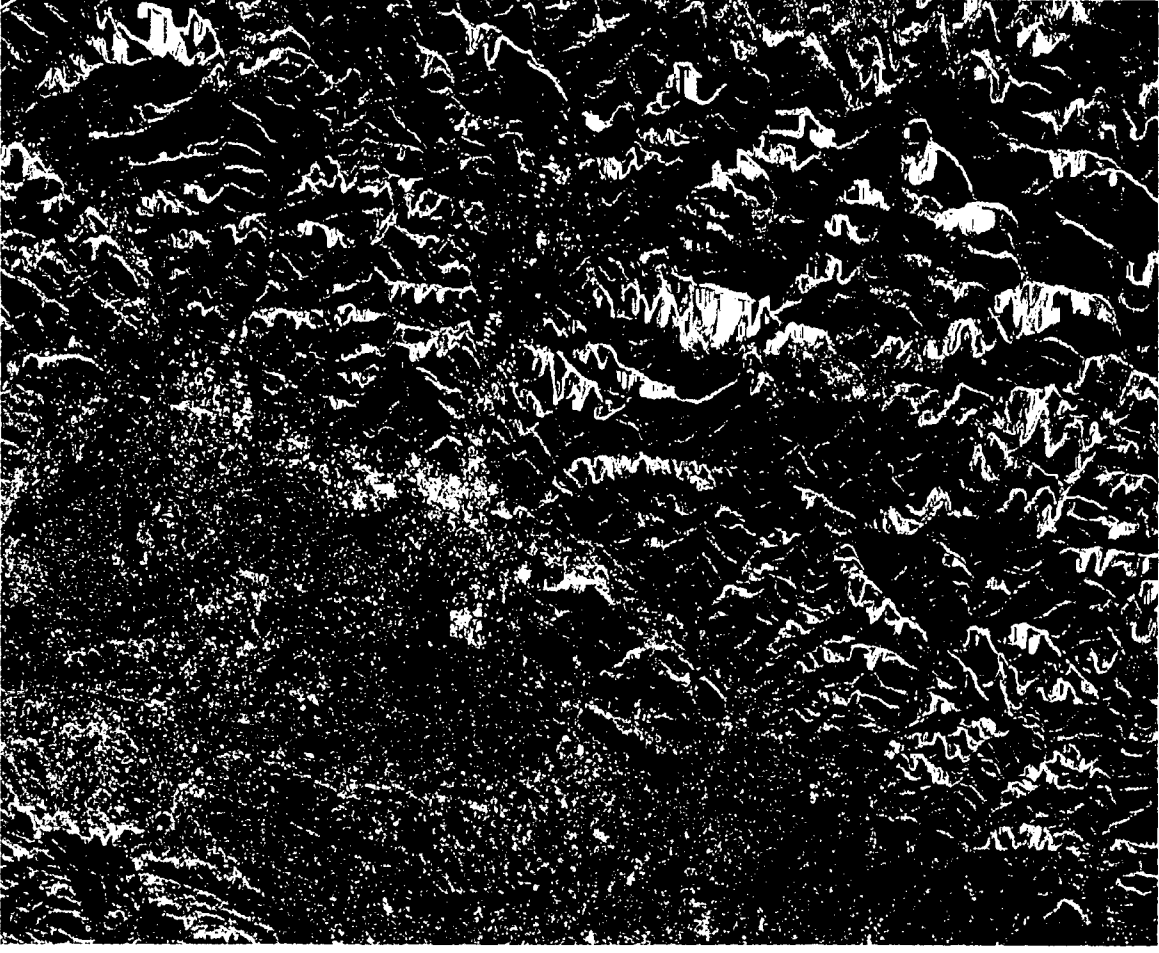


Spot-PAN vertical

Figure 22: Two SPOT-PAN images of the Black Forest. One with vertical viewing and roads correctly registered (left) and one with oblique viewing with the roads displaced in the higher part (right). A DEM is included for clarity.



ERS image not corrected for relief



ERS image corrected for relief

Figure 23: ERS image of a mountainous area. In the left panel the original image is shown. In the right panel an image corrected for relief is shown. The city Freiburg is visible in the centre of the image.

In May 1997 PHARUS was tested above a mountainous area near the city of Freiburg. A restricted area was imaged at an altitude of 5700 meter with an incidence range of 45-65 degrees. The polarimetric image (3 by 6 km) is shown in Fig. 24 where the HH, HV and VV polarisations are shown in the red, green and blue channels. For comparison also a topographic map together with an elevation map and a slope map of the same area are shown.

Black Forest as seen by PHAKUS

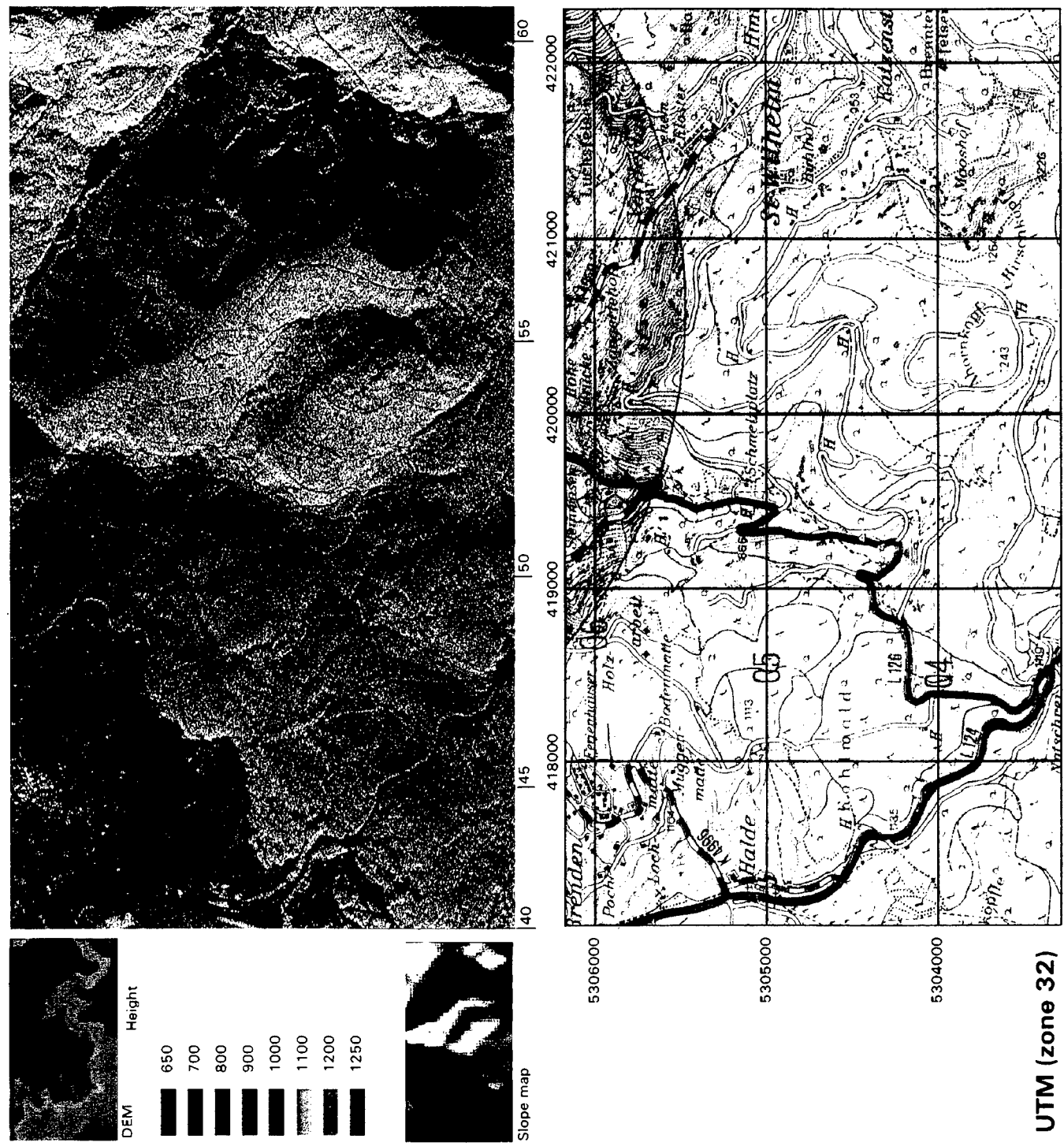


Figure 24: *Polarimetric PHARUS image in the usual colour representation showing a part of the Black Forest. For comparison a topographical map (1:50,000) of the same area is shown. Also shown in smaller frames are a digital elevation model (DEM) and a slope map.*

Because of the large incidence angles the geometrical distortions due to relief are relatively small (see section S1.3.2 of the Technical Supplement). This can also be seen from Fig. 25 where we show an image (VV polarisation only) which has been corrected for relief using the digital elevation model (DTED), which is shown in Fig. 24. The geometrical differences between Fig. 24 and 25 are only small. The biggest distortion is seen to the right where the change in height is considerable.

The radiometric distortions due to relief are however quite distinct. This can be seen by comparing the slope map with the PHARUS image. In the slope image the brightness is proportional to the height gradient towards the radar. Slopes pointing to the radar are bright and slopes pointing away from the radar are dark, where the radar has flown to the left. Since the brightness in the radar image corresponds quite well with brightness in the slope map we can conclude that the relief is the dominant factor determining the backscatter. (i.e. the brightness) The polarimetric information is however less influenced by the relief since the colours do not change considerably with the change in height.

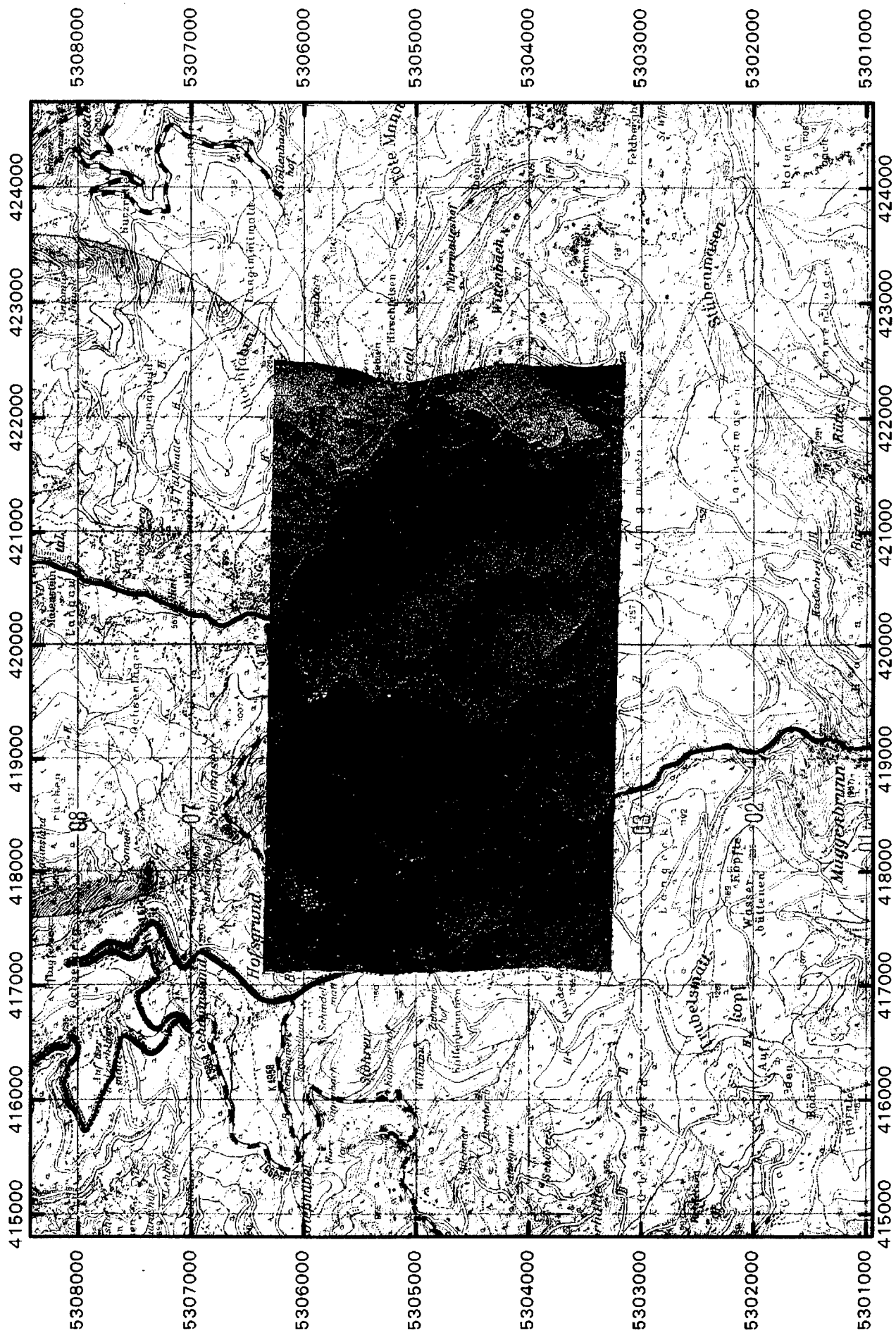


Figure 25: VV polarised PHARUS image geo-registered to the topographical map. Note the distortions at the right of the PHARUS image due to the relief.

5.2 DEM generation from remote sensing images

Optical - stereo

Optical stereo techniques are used since early this century to generate DEMs in a completely manual and analogue process. With the availability of the computer analogue procedures were replaced by an automatic process. In addition stereo imagery from space in fully digital form became available, so that DEMs can easily be generated all over the world.

We demonstrate here the capability of generating DEMs out of spaceborne optical images using a set of stereo SPOT images for the Freiburg test area. The produced DEM can be used for terrain analysis and for the ortho-correction of the satellite imagery. As described in section S1.1.3 of the Technical Supplement the SPOT system is a pushbroom line scanner which can point the sensor away from the track by -27 to +27 degrees.

By using images of the same area, which are acquired from satellite tracks having different viewing directions, a stereo data-set can be obtained. In case the satellite positions and attitudes during image acquisition are known, it is possible to compute the X, Y, Z co-ordinates of a certain point in the terrain when this point can be located in the two images. The measurement of the co-ordinates of the corresponding points in the images and the computation of a DEM is done with software where image matching techniques are implemented, so that only operator interaction is required to evaluate and correct the results. A more detailed description of this process can be found in section S3.2.1 of the Technical Supplement.

Three Spot images of the Freiburg area with viewing directions -29.6°, +00.2°, -25.5° are available (see Table 2, section 2.3). Ideally two images with a difference in viewing direction of at least 25 degrees and with a few days time between the acquisitions should be used. Such image pairs are however not available for the Freiburg test area and only the following image pairs can be formed:

1. A stereo pair of images acquired at 02-07-94 and 04-08-94. The time difference between the images is 1 month. The difference in viewing direction is 29.4 degrees, resulting in a baseline to height (B/H) ratio of 0.55, which is good. The only problem with this data set is the fact that the image of 02-07-94 does have some cloud coverage in the south-eastern part, just where most of the relief is present. At the places with cloud cover no matching can take place and so no elevation data can be extracted.
2. A stereo pair of images acquired at 06-08-91 and 04-08-94. The time difference between the images is three years, which is a long time in which a lot of mutations can have taken place, complicating the image matching process. The season of the year is exactly the same however. The difference in viewing direction is 25.3 degrees, corresponding in a B/H ratio of 0.45 which is still enough. Both images do not show cloud coverage.

It can be concluded that in practice the availability of an appropriate stereo image pair out of the historical database can be a problem. A request can be sent to the satellite operator to acquire such a stereo set, which than normally results in a good pair within a number of weeks, depending on the weather conditions. The planned future optical satellite systems in many cases do have forward-afterward stereo capabilities, which significantly enlarges the possibilities in acquiring appropriate data-sets.

Out of the two SPOT stereo pairs two DEMs were generated, using the Erdas Orthomax software.

The three images were handled in one geometrical model. The co-ordinates of about 50 ground control points were measured in the images and in the 1:50,000 maps. These measurements and the SPOT header data were the input for the triangulation process in which the optimal accurate geometrical relations between the images (relative) and the terrain co-ordinate system (absolute) are determined. The found accuracy of the triangulation process were in the order of 0.8 pixels, or 8 meter, which is good.

In the next step stereo pairs were computed, based on the triangulation parameters. The result of this process turned out to be inaccurate. Deviations of about 20 lines were found. The exact reason for this is not clear at the moment, but probably will be in the header data of the SPOT images.

In order to come to an end-product, it was decided to choose a part of the terrain for which the deviations were still acceptable. The area around the so-called Kaiserstuhl was chosen.

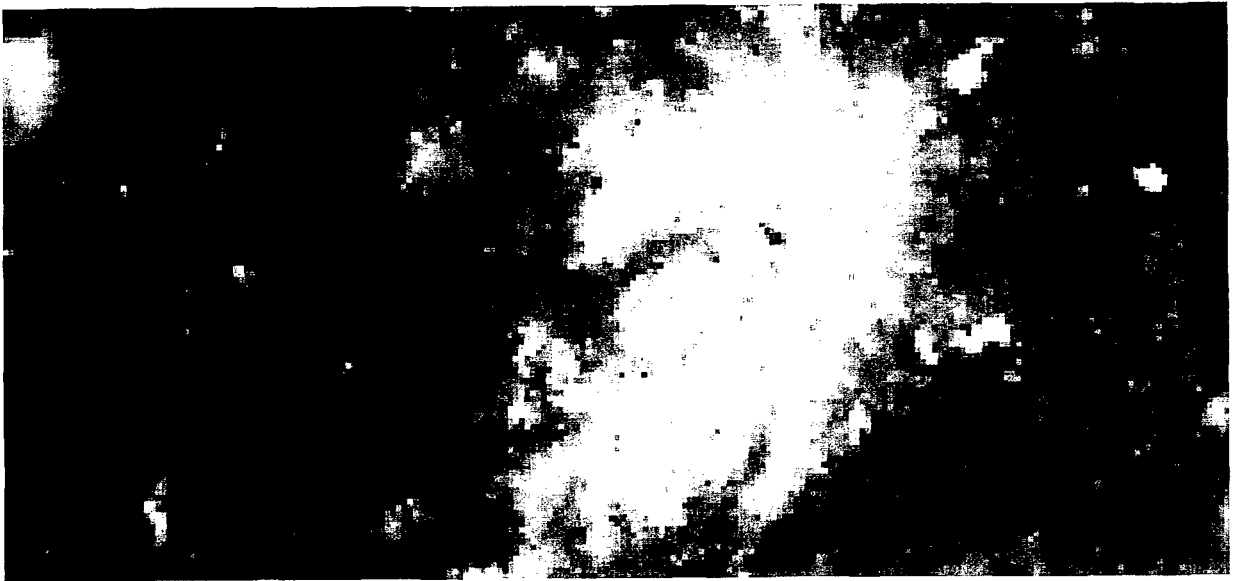
For this area DEMs could be computed using automatic matching techniques. An overview of the Kaiserstuhl area is shown in Fig. 26.



Spot PAN 4-8-94

Figure 26: SPOT-PAN image showing the Rhine valley including the Kaiserstuhl mountain.

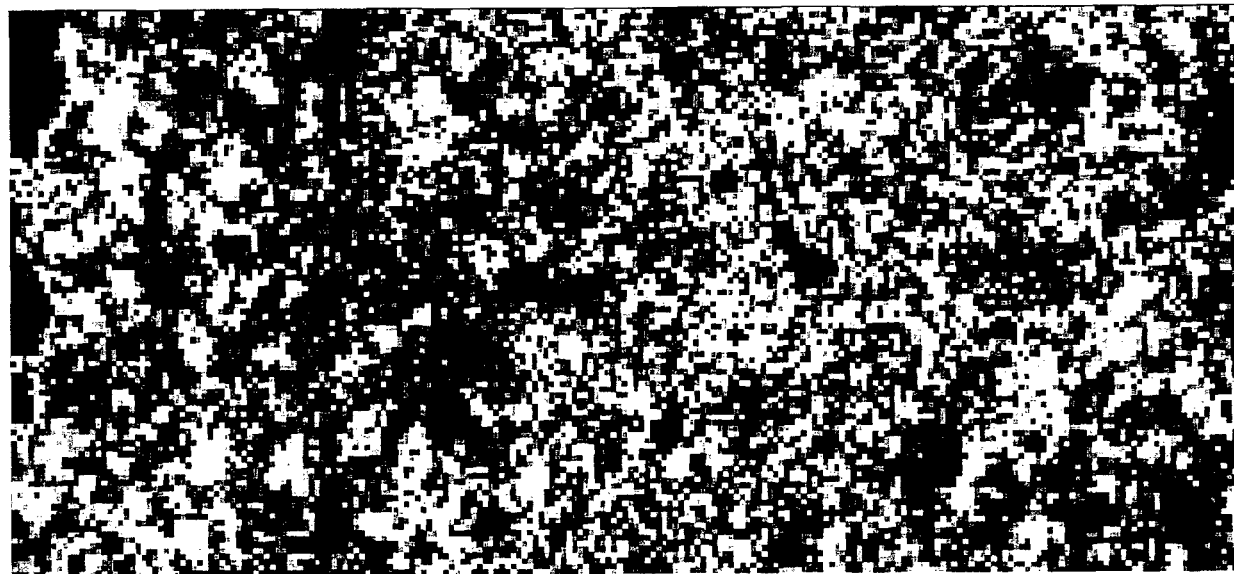
One DEM was generated from the image pair of 02-07-94 and 04-08-94. The DEM was generated with a grid size of 100 x 100 meter. 58% of the DEM grid points could be determined by matching techniques. The matching accuracy of these points is 5.2 meters with a standard deviation of 1.8 meter. The other 42 % of the points need to be interpolated. The large amount of mismatches is caused by the bad geometry of the model (the average y-parallax found in this selected area still amounts to 3.5 lines). Furthermore some parts are covered by clouds, so that no matching was possible. Inspection of the computed DEM showed that at places where cloud cover existed, no matches were found. Especially in forested regions less matching points were found. Manual editing was needed here in order to get a complete good quality DEM. An image of the DEM is shown in Figure 27a as grey-scale image and in Figure 28a as shaded relief.



DEM from Spot 8-91 and Spot 8-94



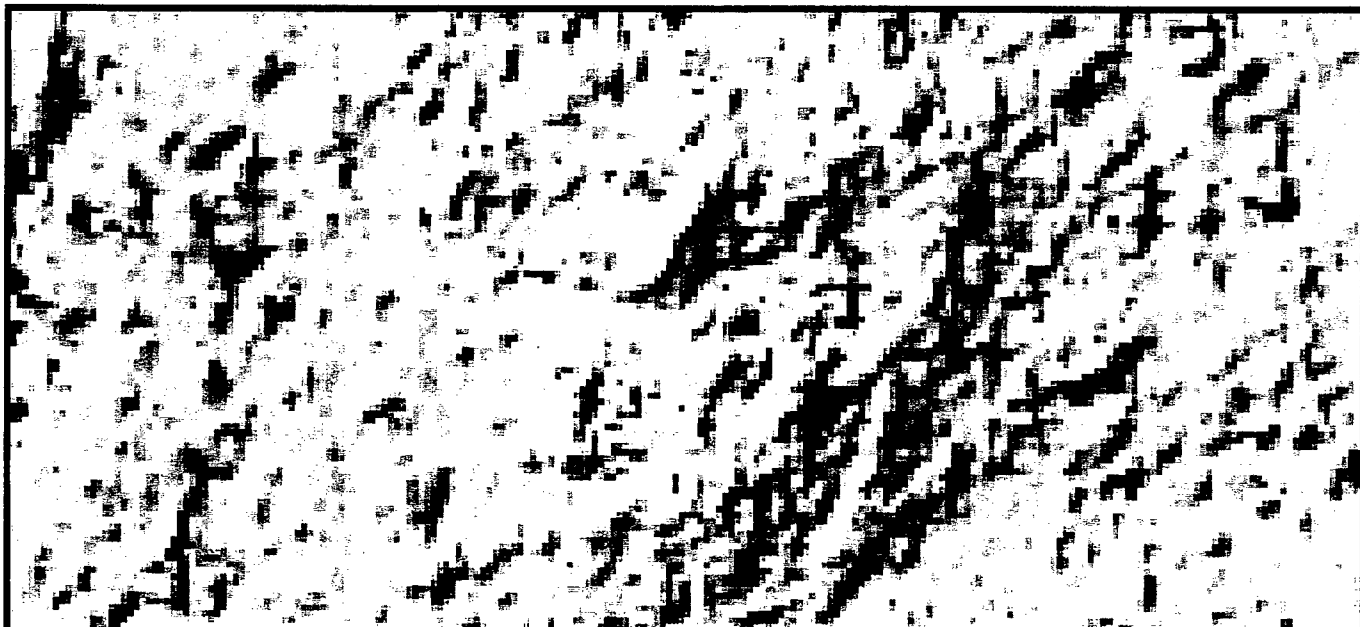
DEM from Spot 7-94 and Spot 8-94



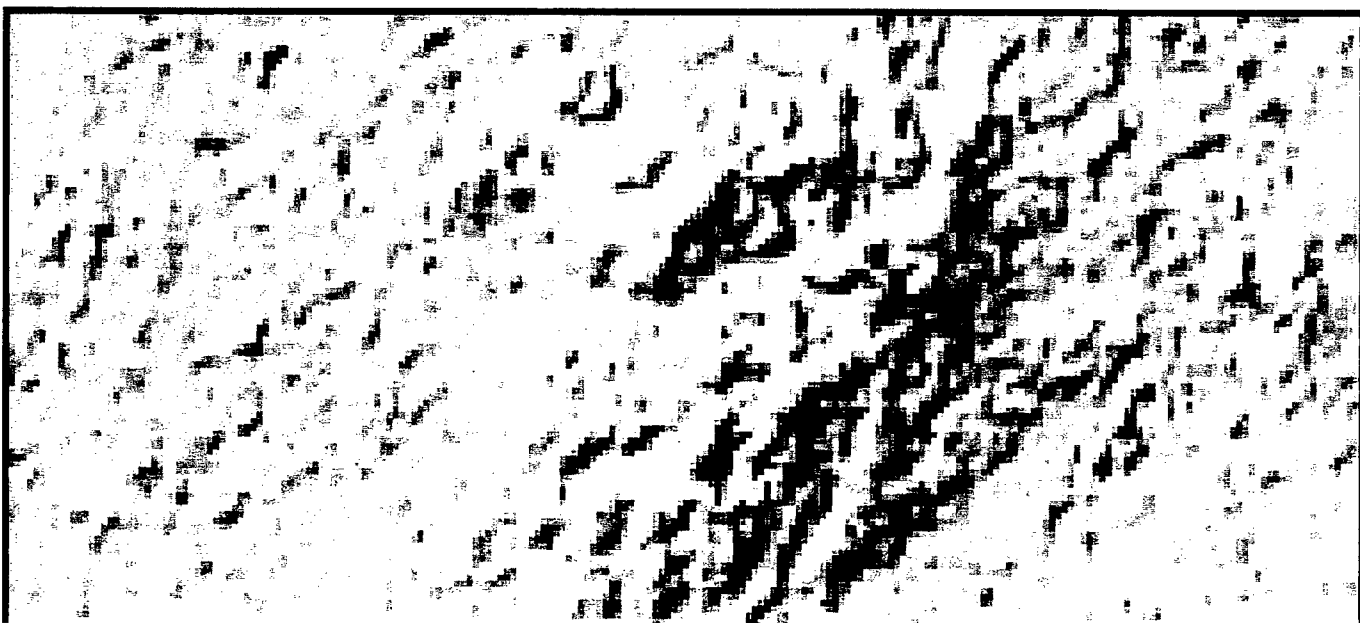
Difference between two DEM's

Figure 27: Figure showing two DEMs (Fig. 27a and 27b) produced from SPOT stereo image pairs of the Kaiserstuhl area and the difference between these DEMs. See text for explanation.

The second DEM was generated from the image pair of 06-08-91 and 04-08-94. The DEM was also generated with a grid size of 100 x 100 meter. 42 % of the DEM grid points could be determined by matching techniques. The rest of the points were interpolated. Because of the long time of three years between the images especially in agricultural areas many changes have taken place, which resulted in little successful matches in these areas. In Figures 27b and 28b where the DEM is shown as a grey scale image and as shaded relief, it can be seen that there exist relative large areas where no points could be determined by matching, leading to inaccurate interpolation results (darker areas). The successful matched points have a mean accuracy of 5.5 meter with a standard deviation of 5.5 meter.



Shaded relief DEM 8-91 and 8-94



Shaded relief DEM 7-94 and 8-94

Figure 28: The same DEM's (Fig. 28a and 28b) as in Fig. 27, but in shaded relief.

The two generated stereo models were compared with each other also, by computing the difference between them. The mean absolute difference is 21.6 meters with a standard deviation of 44.7 meter. 72 % of the points do have a difference of less then 22 meter, 89 % less then 44 meter. In Figure 27c the differences between the two DEMs is shown in colour. The green areas do have a difference less then 33 meter, the yellow from 33 to 67 meter, the red from 67 to 100 meter, and the magenta more then 100 meter.

Despite of the geometrical problems in the data set , the results show a good potential of SPOT stereo data to generate DEMs with accuracies in the order of 10 meters and grid sizes of 100 meters or less.

Microwave - interferometry

As is explained in section S3.2.1 of the Technical Supplement phase differences between two almost identical microwave images can be used to generate a DEM by interferometric techniques.

Two nearly identical images can be obtained by imaging with two radars separated only by a so-called small (in order of about 100 m in space) baseline (single pass interferometry) or by two successive passes of the same radar in almost identical orbits (repeat pass interferometry).

At the moment only repeat pass interferometry from space is possible.

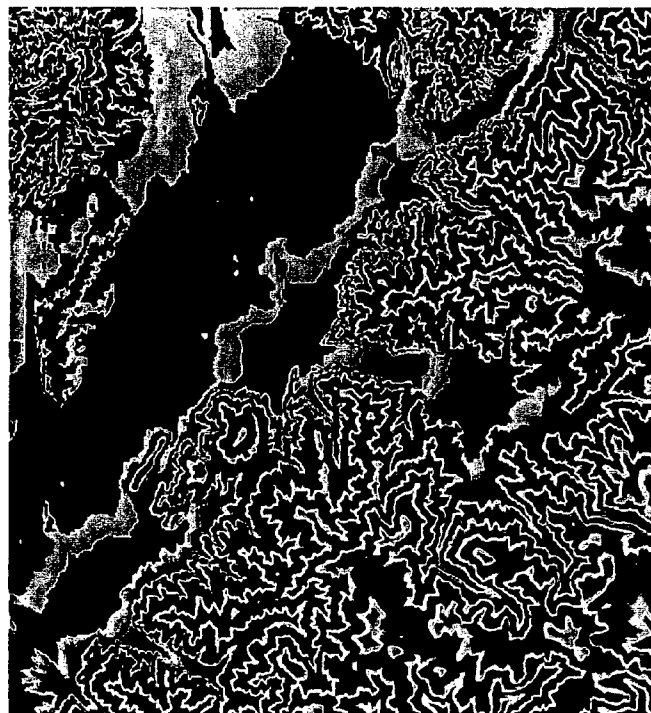
Especially the ERS1/2 tandem mode provides interferometric pairs of images with a temporal separation of one day and a baseline of about 100 meter. The height accuracy of the DEM obtained in this way can be better than 10 meter, depending on the so-called correlation of the images

In Fig. 29 we shown the DEM derived from the ERS1/2 tandem mode compared with the DEM based on DTED. Good agreement is found for the valleys, but not for the more mountainous areas, where the ERS1/2 DEM appears noisy. This is due to the fact that the image pairs do not correlate mostly due to forested areas where small changes occur within one day. Also slopes which are too steep for the range resolution of about 25 meter hinders the generation of a DEM.

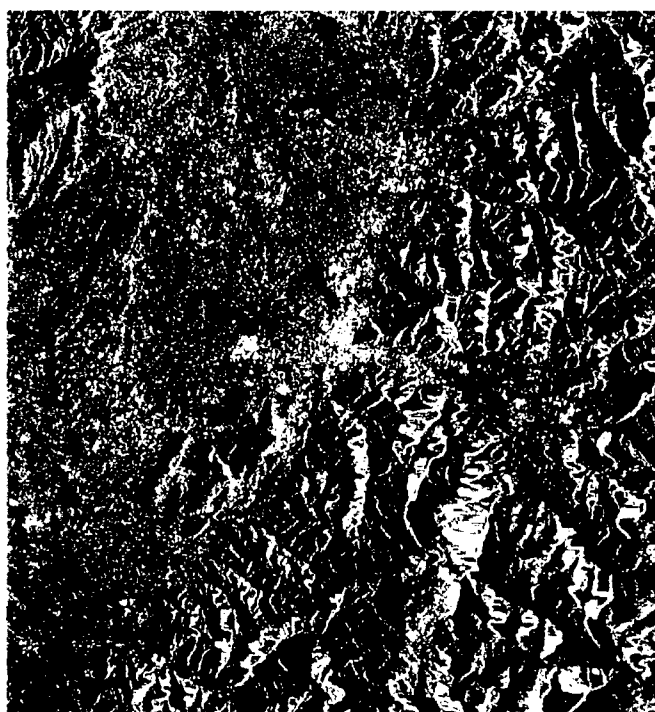
Freiburg area



DEM (ERS1/2)



DEM (DTED)



ERS1 (corrected)



LandSat (RGB: band 5,4,3)

Figure 29: Figure showing a DEM derived from an interferometric ERS1/2 pair of images (top left). For comparison an existing DEM (top right), a for relief corrected ERS image (bottom left) and a LandSat TM image (bottom right) of the same scene are shown.

We can therefore conclude that microwave interferometry in principle can generate an accurate DEM (height resolution $< 10\text{m}$), but that this should be done with single pass interferometric techniques. Also the range resolution should be good (< 10 meter) enough in order to account for the steeper slopes.

In the near future (1999 or 2000) a Space Shuttle flight is planned with two radars separated by a boom of a length of about 60 meter. The data-set obtained will produce in principle a DEM for the whole of the world between 60 degrees Northern and Southern latitude. The height resolution will be about 15 meter posted at 30 meter ground resolution (DTED level II).

6. Conclusions

6.1 General

It is difficult to draw general conclusions for the whole set of features, since the characteristics of the features are quite diverse. Every feature therefore needs to be considered on its own. By grouping the features into classes some general conclusions can be drawn, since many of the 'culture' features are point targets, while the 'land forms/ vegetation' features are often polygons.

In general we can say that most of the features of the DIGEST list in Table 3 can be detected and recognised when the resolution and the wavelength is appropriately chosen. Man-made features like buildings or roads can be detected and often recognised quite adequately when the resolution is appropriate, i.e. less than 5 meter. The recognition of towers is difficult when the viewing direction is vertical. Direct detection of fences and power transmission lines are difficult due to their small dimensions. With resolutions less than 1 meter most features can be recognised. For extended features like crop land or forest spectral information or polarimetric information is more important than the resolution.

Some features like inundation (BH090) and underground water (BH115) are difficult to observe directly with remote sensing sensors. Sometimes information can be obtained indirectly by observing other features which are related (i.e. context information; for example, green vegetation in case of available underground water).

6.2 Comparison between the sensors

Optical sensors make use of daylight and are weather dependent. For optical sensors high resolution images can be obtained, which facilitates the recognition of objects. Radiometric resolution and spectral information are also quite important to discriminate objects, especially between man-made objects and vegetation. Near-infrared information is very useful to discriminate different types of vegetation.

TIR sensors are very suitable to detect and to recognise man-made objects, like buildings, roads etc., when the circumstances are good (i.e. clear and sunny weather). However, the circumstances are very crucial for TIR sensors. During a cloudy, misty or rainy day the contrast vanishes and objects (also man-made objects) are hardly visible in the image. For the discrimination of vegetation types TIR sensors are less suitable.

The main advantage of microwave sensors is that they are independent of most circumstances since they are active sensors which can be used in principle during all weather conditions and at night. Microwave sensors can be appropriate for

detecting objects due to specular reflections which give high returns in the image even when the resolution cell is significantly larger than the object (e.g. high tension pylons in ERS images). The result is a point feature which does not allow recognition. In general the ability of microwave sensors to recognise objects is rather low. Even when more resolution cells are covering the object recognition is difficult since then usually only a collection of points is seen. The contour of the object which is the main feature for recognition in the optical and TIR is in microwaves image suppressed due to the appearance of specular reflections and speckle.

The low resolution of present-day spaceborne sensors is clearly disadvantageous for obtaining geographical information.

6.3 Context

A quite important concept for detection and recognition is 'context information'. As is defined in the reference list (Appendix) the context can provide information about a feature even when the feature cannot be observed directly. Since in many cases features show up as small objects in the image only a few pixels provide information limiting the recognition. However other independent information available for the interpreter, for example background information about location and the surroundings can provide the essential information so that recognition or even identification becomes possible. This so-called 'context information' will always play an important role in using remote sensing images.

6.4 Relief

We conclude that due to relief images both in the optical as well as in the microwave domain are usually distorted. Only when the look direction is vertical no distortions are present. This is not applicable to the microwave domain since the radar is always side-looking in order to acquire images. The distortions can in principle be used in stereo pairs of images to extract height information and to produce a digital elevation model (DEM). The results of the present work indicates that SPOT stereo data has a good potential to generate DEMs with accuracies in the order of 10 meters and grid sizes of 100 meters or less.

Appropriate optical stereo image pairs are not always available from historical databases, but can be obtained from present spaceborne systems within a number of weeks, depending on the weather conditions, however. Future planned optical satellite systems often will have forward-afterward stereo capabilities, so that stereo pairs can be acquired during one over pass, which significantly enlarges the possibilities for acquiring appropriate data-sets.

Microwave interferometric image pairs can in principle also generate accurate DEMs (height resolution < 10m), but it is clear that this should be done with single

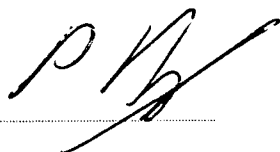
pass interferometric techniques. Also resolutions should be higher than present day microwave spaceborne systems in order to account for the steeper slopes.

In the near future (1999 or 2000) a Space Shuttle flight is planned with two radars separated by a boom of a length of about 60 meter, which satisfies most of these conditions. It is expected that a world wide DEM between 60 degrees Northern and Southern latitude will be acquired with a height resolution of about 15 meter posted at 30 meter ground resolution (DTED level II).

7. References

- [1] Broek van den A.C, Data-acquisitie t.b.v. GIS, 1994, TNO rapport, FEL-94-A286.
- [2] Consalez, R.C., R.E. Woods, Digital Image Processing, 1993, Addison-Wesley.
- [3] DIGEST FACC (Digital Geographical Information Exchange Standard, Features and Attributes Coding Catalogue), 1992, Digital Geographical Information Working Group, Department of National Defence of Canada and the Defence Mapping Agency, USA.
- [4] Fundamentals and Special Problems of Synthetic Aperture Radar (SAR), AGARD Lecture Series 182, 1992.
- [5] Hees, van G.S., Globale en Lokale Geodetische Systemen, 1994, Nederlandse commissie voor geodesie, Delft.
- [6] Jacobs, P.A., Thermal Infrared Characterisation of Ground Targets and Backgrounds, 1996, Tutorial Texts in Optical Engineering, Vol. TT26, Spie Optical Engineering Press.
- [7] Kiefer, R.W., T.M. Lillesand, Remote Sensing and Image Interpretation, 1987, John Wiley and Sons.
- [8] Kramer, H.J., Observation of the Earth and Its Environment, Survey of Missions and Sensors, 1996, Springer-Verlag.
- [9] Laanen, M.L., Onderzoek naar de mogelijkheden van geografische data-acquisitie met behulp van optische en radar remote sensing beelden, 1996, TNO rapport, FEL-96-S200.[9] Remote Sensing: A Valuable Source of Information, AGARD Conference proceedings 582, 1996.
- [10] Richards, J.A., Remote Sensing Digital Image Analysis, 1993, Springer-Verlag.
- [11] Ulaby, F.T., R.K. Moore, A.K. Fung, Microwave Remote sensing, Vol. I-III, 1982, Addison-Wesley.
- [12] TERAS, Eindrapport Terrein Analyse Systeem, 1995, Werkgroep Militaire Geografie, Koninklijke Landmacht.
- [13] Wijnhoud, J.D., Het gebruik van remote sensing en GIS t.b.v. inventarisatie en analyse van terrein en bodem voor militaire doeleinden, 1995, TNO rapport, FEL-95-S287.

8. Signature

A handwritten signature in black ink, appearing to be 'P. Hooijboom', written over a horizontal line.

P. Hooijboom
Group leader

A handwritten signature in black ink, appearing to be 'Dr A.C. van den Broek', written over a horizontal line.

Dr A.C. van den Broek
Project leader/Author

ONGERUBRICEERD

REPORT DOCUMENTATION PAGE
(MOD-NL)

1. DEFENCE REPORT NO (MOD-NL) TD98-0169	2. RECIPIENT'S ACCESSION NO	3. PERFORMING ORGANIZATION REPORT NO FEL-98-A077
4. PROJECT/TASK/WORK UNIT NO 25039	5. CONTRACT NO A95KL756	6. REPORT DATE August 1998
7. NUMBER OF PAGES 94 (excl RDP & distribution list)	8. NUMBER OF REFERENCES 13	9. TYPE OF REPORT AND DATES COVERED Final
10. TITLE AND SUBTITLE Geographical information extraction with remote sensing Part I of III - Main report		
11. AUTHOR(S) Dr A.C. van den Broek, M. van Persie, H.H.S. Noorbergen, Dr G.J. Rijckenberg		
12. PERFORMING ORGANIZATION NAME(S) AND ADDRESS(ES) TNO Physics and Electronics Laboratory, PO Box 96864, 2509 JG The Hague, The Netherlands Oude Waalsdorperweg 63, The Hague, The Netherlands		
13. SPONSORING AGENCY NAME(S) AND ADDRESS(ES) KMA		
14. SUPPLEMENTARY NOTES The classification designation Ongerubriceerd is equivalent to Unclassified, Stg. Confidentieel is equivalent to Confidential and Stg. Geheim is equivalent to Secret.		
15. ABSTRACT (MAXIMUM 200 WORDS (1044 BYTE)) <p>The goal of this study is to evaluate the potential of remote sensing for geographical information extraction. We have therefore collected remote sensing data from sensors in different wavelength regions (optical, thermal infrared and microwave) and for two test sites showing a variety of geographical features. The extracted geographical information has been compared with an existing ground database (TERAS) using a selected DIGEST feature list.</p> <p>With resolutions of about 5 meter most features can be detected and with resolution less than 1 meter most features can be recognised. For extended features like crop land or forest spectral or polarimetric information is more important than the resolution.</p>		
16. DESCRIPTORS Remote sensing Sensor fusion Mapping		IDENTIFIERS Geographical information extraction Multi wavelength
17a. SECURITY CLASSIFICATION (OF REPORT) Ongerubriceerd	17b. SECURITY CLASSIFICATION (OF PAGE) Ongerubriceerd	17c. SECURITY CLASSIFICATION (OF ABSTRACT) Ongerubriceerd
18. DISTRIBUTION AVAILABILITY STATEMENT Unlimited		17d. SECURITY CLASSIFICATION (OF TITLES) Ongerubriceerd

Distributielijst

1. DWOO
2. HWO-KM*
3. HWO-KL
4. HWO-KLu*
5. HWO-CO*
6. KMA, t.a.v. Ir. J. Rogge
7. DM&P TNO-DO
8. Directeur TNO-PML*
9. Directeur TNO-TM*
10. Accountcoördinator KL*
- 11 t/m 13. Bibliotheek KMA
14. HQ 1 (GE/NL) Corps G-2 Division (MilGeo), NL Topo Offr
15. Staf 1 (NL) Divisie H-Sie G2
16. C-101 MI peloton
17. Wing Mission Planning Vlb. Volkel, Maj. J.W. van den Heuvel
18. Chef der Hydrografie, G. Spoelstra
19. Militaire Inlichtingendienst, Afd. Inl., Dr. L.H.P. Meijer
20. Genie OC, Hfd Kenniscentrum
21. KMA, Ir. J. Schellekens
22. NLR, Ir. M. van Persie
23. NLR, Ing. H.H.S. Noorbergen
24. NLR, Dr. G. van den Burg
25. TDN, Ir. P. van Asperen
26. TDN, Ir. E. Kolk
27. LAS/BO/OB, Lkol. A. Dondorp
28. DMKL/T&WO, Ir. N Pos
29. DMKM/WCS/COSPON, Drs. W. Pelt
30. DOPKLu, Ir. S.J.J. de Bruin
31. DMKLu/MXS, Ir. G. de Wilde
32. MID-KL, bureau MilGeo, Maj. A. Schoonderbeek
33. MID-KL, bureau MilGeo, Maj. R.J.T. Veltman
34. MID-KL, bureau MilGeo, Kap. G.L. Weerd
35. OCEDE/KCEN/SMID, Hfd sectie plannen, Lkol. G.F. van Kempen
36. OCEDE/KCEN/SMID, Maj. M. van Ommen Kloeke
37. OCEDE/KCEN/SMID, H. Ebbers
38. Directeur TNO-FEL
39. Adjunct-directeur TNO-FEL, daarna reserve
40. Archief TNO-FEL, in bruikleen aan MPC*
41. Archief TNO-FEL, in bruikleen aan Accountmanager KL*
42. Archief TNO-FEL, in bruikleen aan Ir. P. Hoogeboom
43. Archief TNO-FEL, in bruikleen aan Dr. A.C. van den Broek
44. Archief TNO-FEL, in bruikleen aan Dr.ir. G.J. Rijckenberg
45. Archief TNO-FEL, in bruikleen aan Ir. P.J. Schulein
46. Archief TNO-FEL, in bruikleen aan Ir. C.J. den Hollander
47. Archief TNO-FEL, in bruikleen aan Ir. V.F. Schenkelaars
48. Archief TNO-FEL, in bruikleen aan G.D. Klein Baltink
49. Archief TNO-FEL, in bruikleen aan Drs. E. van Halsema
50. Archief TNO-FEL, in bruikleen aan Drs. J.K. Vink
51. Archief TNO-FEL, in bruikleen aan Ing. D. Kloet
52. Archief TNO-FEL, in bruikleen aan Drs. J.S. Groot
53. Documentatie TNO-FEL
54. Reserve

Indien binnen de krijgsmacht extra exemplaren van dit rapport worden gewenst door personen of instanties die niet op de verzendlijst voorkomen, dan dienen deze aangevraagd te worden bij het betreffende Hoofd Wetenschappelijk Onderzoek of, indien het een K-opdracht betreft, bij de Directeur Wetenschappelijk Onderzoek en Ontwikkeling.

* Beperkt rapport (titelblad, managementuittreksel, RDP en distributielijst).